A Framework for Efficient Trajectory Comparisons in the Earth-Moon Design Space

Davide Guzzetti*, Natasha Bosanac*, Kathleen C. Howell†
Purdue University, Armstrong Hall of Engineering, 701 W. Stadium Ave., West Lafayette, IN 47907-2045
and David C. Folta ‡
NASA Goddard Space Flight Center, Greenbelt, MD, 20771, USA.

The development of a blueprint for a long-term human presence in the Earth-Moon space, crewed and robotic, currently retains significant interest in orbital destinations that include the vicinity of the libration points, as well as other trajectories that exist within a multi-body dynamical environment. The concept of an interactive and "dynamic" catalog of potential solutions in the Earth-Moon system is explored and analyzed as an efficient framework to guide trajectory design. The catalog concept is practically implemented in the form of a graphical user interface. Examples demonstrating applications to preliminary mission design offer rapid and effective strategies for orbit comparison and selection within a multi-body regime.

I. Introduction

Despite some visionary missions that have extended robotic space exploration beyond the borders of the solar system, actual and stable human space settlements are currently and consistently active only in Low-Earth Orbits (LEO). For the development of a blueprint for a more permanent and long-term human presence in the Earth-Moon space, crewed and robotic, a more comprehensive and easily accessible "roadmap" of destinations and pathways throughout Earth-Moon neighborhood is a critical component. The regions near the libration points, as well as other trajectories that exist within a multi-body dynamical environment, retain significant interest. In fact, these types of dynamical structures prove to be a versatile framework for mission design. In recent years, many NASA-released studies have considered such alternative trajectory platforms for long-duration infrastructures to support science in the Earth-Moon region, to serve as gateways to other interplanetary destinations, to support lunar orbit and surface operations and to assist deep space telescopes.[1,2,3] Most recently, both the 2013 Global Exploration Roadmap[4] and the 2014 National Research Council report on human space exploration[5] include additional mission concepts, e.g., travel to Mars and rendezvous with asteroids, that also leverage the dynamics associated with the equilibrium points of the Earth-Moon system. Altogether, this scenario suggests that broader knowledge of the dynamical accessibility within the Earth-Moon system is warranted.

Over the last few years, the success of many Sun-Earth libration point missions has positively contributed to the large rise in interest of the three-body problem. The Acceleration, Reconnection, Turbulence and Electrodynamics of the Moons Interaction with the Sun (ARTEMIS) mission also demonstrated that three-body analyses are viable options for trajectory design in the Earth-Moon neighborhood.[6] Along with these accomplishments, the mathematical foundations in the three-body problem are now better understood and more often exploited, frequently due to the dynamical systems approaches. Consequently, a large number of solutions and techniques have been developed and consolidated by the astrodynamics community that might be employed for orbit design and operation. Many software packages, for example, Satellite Tool Kit

*Ph.D. Student, School of Aeronautics and Astronautics, Purdue University, Armstrong Hall of Engineering, 701 W. Stadium Ave., West Lafayette, IN 47907-2045.
†Hsu Lo Distinguished Professor, School of Aeronautics and Astronautics, Purdue University, Armstrong Hall of Engineering, 701 W. Stadium Ave., West Lafayette, IN 47907-2045. Fellow AAS; Fellow AIAA.
‡Senior Fellow, NASA Goddard Space Flight Center, Greenbelt, MD, 20771, USA.

(STK) and NASA's General Mission Analysis Tool (GMAT), offer a graphical environment for trajectory design incorporating gravitational fields at various levels of fidelity.[7,8] However, the focus of these packages is generally directed towards the delivery of trajectory designs and other actual mission support capabilities. Thus, they offer limited guidance and insight into the available dynamical structures throughout the region; a comprehensive design procedure to easily incorporate and leverage the three-body dynamical structures has not yet been completely established. The current effort is devoted to creating direct links between the problem understanding and its practical application by exploring the Earth-Moon design space. There exists a wide array of known orbits with significant potential for parking, staging and transfers within the Earth-Moon system. Software such as AUTO can supply a selection of these solutions as well as some insight into the local dynamics and the evolution of a set of orbits along any family.[9] Nonetheless, mission designers currently lack a basic "blueprint" to support rapid, efficient and well-informed decisions regarding the use of these known periodic orbits for any mission prior to an end-to-end trajectory design. Typically, the most basic trade-offs in path planning are not intuitive and, yet, not easily accessible.

The concept of a "dynamic" framework, as opposed to a static database, is explored to guide the preliminary selection of trajectories in a highly sensitive and rapidly evolving design space. A static database can not effectively encompass all the solutions available in the dynamical environment. First, the dynamical structure in the Earth-Moon system, which is represented in terms of the Circular Restricted Three Body Problem (CR3BP), is comprised of a pool of infinitely many solutions, currently without an analytical closed-form description. Second, it is unlikely that a trajectory or group of trajectories could be uniquely represented by a set of parameters that also retain intuitive physical meaning, as in the Keplerian regime. Third, the on-going investigation of the problem from the scientific community allows for the possibility of discovering new periodic orbits or updating the understanding of existing solutions. The capability to compute 'on-demand' solutions and manipulate data through graphical interfaces is available with modern computational tools; accordingly, the concept of a "dynamic" catalog is introduced. Specifically, a "dynamic" catalog is based upon an interactive environment and characterizes the design space also in terms of the trade-offs between various parameters of significance for mission design, rather than relying only on a static classification of solutions. In this way, the "dynamic" catalog may overcome some of the challenges associated with constructing a trade space to analyze the various characteristics of a large set of solutions and their neighboring dynamical behavior.

The construction of a design framework to deliver the desired functional capabilities originates from the identification of parameters that may aid in trajectory design and selection. Quantities of interest may include size, period, energy, and stability. Representative operational costs, such as station-keeping maneuver ΔVs, orbit insertion maneuver magnitude and flight time for transfers from LEO may also be useful. Then, known periodic and quasi-periodic orbits that are solutions in a circular restricted three-body model of the Earth-Moon system, and closely approximate the true dynamical structure, should be incorporated into the catalog. Such selections currently include two-dimensional and three-dimensional orbit families of libration point orbits, direct retrograde orbits about the Moon (DROs), direct prograde orbits about the Moon (DPOs), as well as resonant orbits. The catalog adopts a preliminary classification of orbits into groups, or families, that are well-established in the literature; however, such taxonomy is not definitive, as it must evolve to accommodate new solutions and/or better understanding of links between existing members. The families included in the catalog can also be statistically described in terms of the representative parameters; the statistics are computed on a dataset of periodic orbits sampled along each family. The statistical description aims to create a concise tradeoff space. Moreover, compiling this information in an interactive environment, the orbits can be filtered and compared to identify candidate solutions that potentially satisfy a given set of mission requirements. Eventually, such a framework may offer faster and more efficient strategies for orbit design and operation, while also delivering innovative mission design parameters for further examination, for example, in GMAT or the Adaptive Trajectory Design (ATD) software created at Purdue University,[10] or other end-to-end mission design tools.

In this investigation, the CR3BP model is employed to approximate the dynamical structure of the Earth-Moon system. Based upon the understanding of the CR3BP, the essential concepts to construct a design framework in the Earth-Moon system are presented. As previously noted, the form proposed for the design framework is a "dynamic" catalog of reference solutions in the Earth-Moon system that is implemented as a graphical interactive interface. Accordingly, a catalog interface prototype is developed. To demonstrate that rapid and efficient trajectory comparisons are achievable through the catalog, the interactive interface prototype is applied to some representative scenarios within the context of trajectory design application for

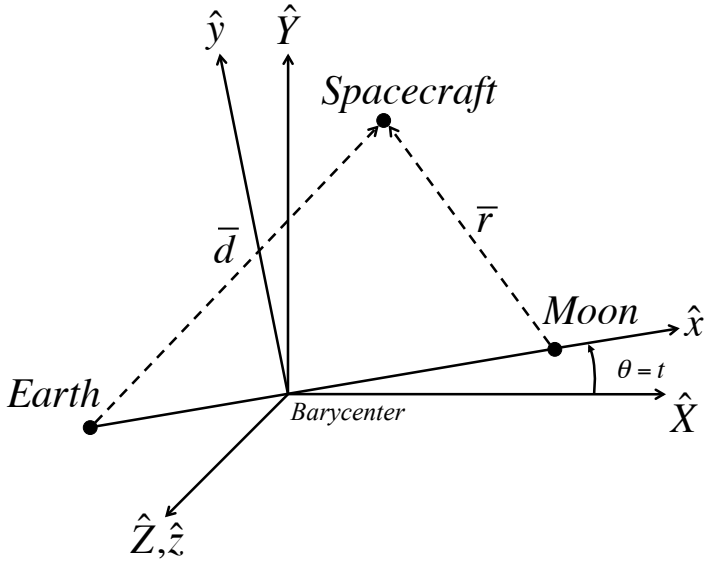

Figure 1. Definition of the rotating coordinate frame with a constant angular velocity relative to the inertial frame at a nondimensional rate of unity about the $\hat{Z}$-axis

the Earth-Moon system.

II. Dynamical Background

To facilitate rapid and intuitive exploration of the dynamical structure in the Earth-Moon system, the circular restricted three-body problem is employed. This dynamical model, which serves as a reasonable approximation to the actual gravitational field, reflects the motion of a massless spacecraft under the influence of the point-mass gravitational attractions of the Earth and Moon. These two primary bodies are assumed to move in circular orbits about their mutual barycenter. The configuration of this system is depicted in Figure 1 using a coordinate frame, $\hat{x}\hat{y}\hat{z}$, that rotates with the motion of the Earth and Moon. In this frame, the spacecraft is located by the nondimensional coordinates (x, y, z). By convention, quantities in the CR3BP are nondimensionalized such that the Earth-Moon distance is equal to a constant value of unity and their mean motion is also equal to one. In addition, the Earth and Moon have nondimensional masses equal to $1-\mu$ and μ, respectively, where μ equals the mass ratio between the actual mass of the Moon and the total mass of the system. In the rotating frame depicted in Figure 1, the equations of motion for the spacecraft are written as:

$$\ddot{x} - 2\dot{y} = \frac{\partial U}{\partial x}, \qquad \ddot{y} + 2\dot{x} = \frac{\partial U}{\partial y}, \qquad \ddot{z} = \frac{\partial U}{\partial z} \tag{1}$$

where the pseudo-potential function, $U = \frac{1}{2}(x^2+y^2) - \frac{1-\mu}{d} + \frac{\mu}{r}$, $d = \sqrt{(x+\mu)^2+y^2+z^2}$ and $r = \sqrt{(x-1+\mu)^2+y^2+z^2}$. This gravitational field admits five equilibrium points: the collinear points L_1, L_2 and L_3, located along the Earth-Moon line; two equilateral points, L_4 and L_5, form equilateral triangles with the two primaries. Since the CR3BP is autonomous, a constant energy integral exists in the rotating frame and is equal to the Jacobi constant, JC:

$$JC = 2U - \dot{x}^2 - \dot{y}^2 - \dot{z}^2 \tag{2}$$

At any specific value of the Jacobi constant, there are infinite possible trajectories exhibiting a wide array of behaviors. However, any trajectory may be generally classified as one of four types of solutions: equilibrium point, periodic orbit, quasi-periodic orbit, and chaotic motion. Each of these solutions can be identified using numerical techniques and subsequently characterized using concepts and quantities from dynamical systems theory.

III. Background for a Dynamic Catalog

To construct a simple catalog for efficiently guiding trajectory design, particular solutions in the form of periodic orbits are exploited. Within the framework of the CR3BP, periodic orbits exist in families and form an underlying dynamical structure. The characterization and classification of such solutions could serve as a guide to select orbits and arcs that may be incorporated along trajectories intended to satisfy a given set of mission requirements. For this investigation, orbital parameters are defined, operational costs are estimated and orbits are organized into families or groups of families that share a common dynamical origin. These concepts are necessary to form the basis of a efficient design framework within any celestial system.

III.A. Orbital Parameters

For a viable description of trajectories within the three-body regime, some Keplerian parameters might be useful. However, their application within a preliminary design framework is limited, particularly concerning two issues: first, such parameters are not uniquely defined, but depend on the primary body assumed as the reference; second, the Keplerian elements are not constant along arcs in a multi-body gravitational environment. No set of analytical constants exist in the CR3BP. However, alternative quantities can be introduced to capture significant features of the periodic orbits within the CR3BP and to preliminarily assess the fulfilment of the mission requirements. A summary of orbital parameters that may be effectively employed in a "dynamic" catalog is reported in Table 1, along with a sample application. The amplitude

Table 1. Orbital Parameters for Periodic Orbits within the CR3BP

Parameter	Interpretation	Sample application
A_x, A_y, A_z	Geometrical amplitude of orbit	Line-of-sight constraints
Period	Time Scale	Maneuvers, communications planning
JC	Energy level	Transfer cost estimation
Stability Index	Orbital stability	Periodic orbit insertion and maintenance

of the periodic orbit in each of the coordinate directions corresponding to the rotating frame $\hat{x}$, $\hat{y}$, $\hat{z}$ is denoted by A_x, A_y, A_z. These amplitudes are numerically calculated as the absolute value of the maximum excursion in the respective positive direction. The amplitudes A_x, A_y, A_z may supply an early estimate of the orbit size, prior to more computationally intensive explorations. Such information might be useful, for example, in the selection of parking orbits when limitations on the communications infrastructure constrain the line-of-sight with respect to either the Earth or Moon.[20] Next, the orbital period is defined as the minimal time for the motion of a spacecraft to repeat in all the specified state variables as viewed in the rotating frame. The orbital period defines the time scale not only along the periodic orbit, but also within neighbouring dynamics. Consequently, this parameter may be employed in operations planning and time-of-flight evaluations. An energy-like quantity is supplied by the Jacobi constant JC, as defined in Eq. (2): the lower the value of Jacobi constant, the more energetic the orbit. By setting an energy level corresponding to each natural trajectory, the Jacobi constant produces a rough estimate for the transfer cost between different periodic orbits. In fact, the cost of any maneuver results from a change of the velocity magnitude (which effectively is a variation in the energy level) and/or a change of the velocity direction. Thus, the transfer cost between two periodic orbits at different JC value must, at the minimum, allow for the energy change, i.e., the adjustment of the Jacobi constant value, while the velocity direction change is neglected. Orbital stability information can also be encapsulated in a scalar metric, i.e., the stability index. According to Floquet theory, the linear stability information relative to a periodic orbit is contained in the eigenvalues of the state transition matrix propagated for one orbital period, i.e., monodromy matrix. The eigenvalues reflect the stability of the nonlinear solution, computed from a local linear approximation for the dynamics in vicinity of the reference orbit. In the CR3BP, six eigenvalues are associated with each periodic orbit: two trivial eigenvalues equal to unity that indicate periodicity, and two reciprocal pairs of eigenvalues. To simplify visualization of the eigenvalues corresponding to a periodic orbit, a stability index, s, is defined. This quantity is set equal to $s = \frac{1}{2}\left(\lambda_{max} + \frac{1}{\lambda_{max}}\right)$, where $\lambda_{max} = \max|\lambda_i|$ denotes the magnitude of the dominant eigenvalue. A stability index with absolute magnitude equal to one identifies marginally stable behaviour, which corresponds to a family of quasi-periodic motion in the vicinity of the periodic orbit. Although quasi-periodic orbits do not repeat over time, they traces out the surface of a torus. In combination with small

maintenance maneuvers, such boundedness might be approximately retained when a quasi-periodic orbit is transitioned into a higher-fidelity gravitational environment. Conversely, a stability index greater than one reflects unstable motion in vicinity of the reference orbit. From such orbits emanate stable and unstable manifolds which may be leveraged to access various regions of the Earth-Moon space via low-cost transfers.

III.B. Classification of Periodic Orbits

Infinitely many types of periodic orbits exist within the CR3BP, and a vast array of such solutions is already available. Categorizing the known orbits into families and classes may serve as a reference base to quickly construct mission scenarios. Even if a static taxonomy is not sufficient to provide an efficient framework for assembling trajectories within the Earth-Moon system, it is still a desirable feature for an interactive and "dynamic" design environment. Such a capability is especially important for users not familiar with the intricacies of the CR3BP and the connections between various types of orbits and their respective families.

Within the CR3BP, a unique characterization of solutions is seldom possible: first, orbits are often computed via numerical algorithm, thus, any complete analytical set of constants that defines the solution remains nonexistent; second, the orbit characteristics may vary significantly, and nonlinearly, across the same group of orbits; and, third, the orbit characteristics may vary continuously across groups of orbits that are linked through a bifurcation of the local dynamics. Accordingly, different classifications are proposed as the understanding of fundamental structures in the CR3BP advances. In this investigation, the classification is based on the conventions most currently accepted in the astrodynamics community, also allowing for a certain margin of flexibility, one that is necessary to accommodate future discoveries and a better understanding of the problem. Orbits are organized into families and families into classes. Members of the same family share the continuous variation of certain parameters and they can be generated through dynamical continuation algorithms. Next, families that trace back to the same dynamical principle of origin are gathered into different classes. Thus, the taxonomy displayed in Figure 2 emerges. The families of periodic orbits are currently organized into four classes: Libration Point Orbits, Resonant Orbits, Moon-Centered Orbits, and Earth-Centered Orbits. Each class is comprised of orbits identified by the boxes corresponding to each orbit family, which can encompass both two-dimensional and three-dimensional members. Although all members of any periodic orbit family may not belong exclusively to one class or one family, as indicated by the black arrows, an intuitive categorization may expedite the search for a desired solution without precise knowledge of its name, shape or evolution.

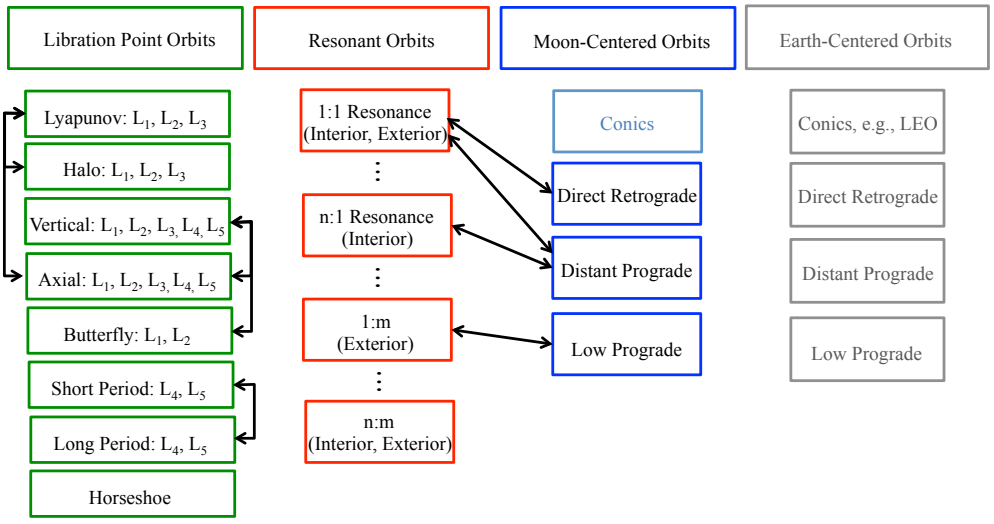

Figure 2. Organization of orbit families included in the reference catalog to date, with selected links indicated; the framework is easily expanded as new options emerge.

Libration point orbits emanate from both the collinear and equilateral libration points. Lyapunov and halo orbits, which are likely the most well-known among the families within the CR3BP, belong to this class. Sample members of these and other families of libration point orbits appear in Figure 3(a), emanating from the L_1 equilibrium point. Libration Points Orbits grant parking options in many regions of the Earth-Moon

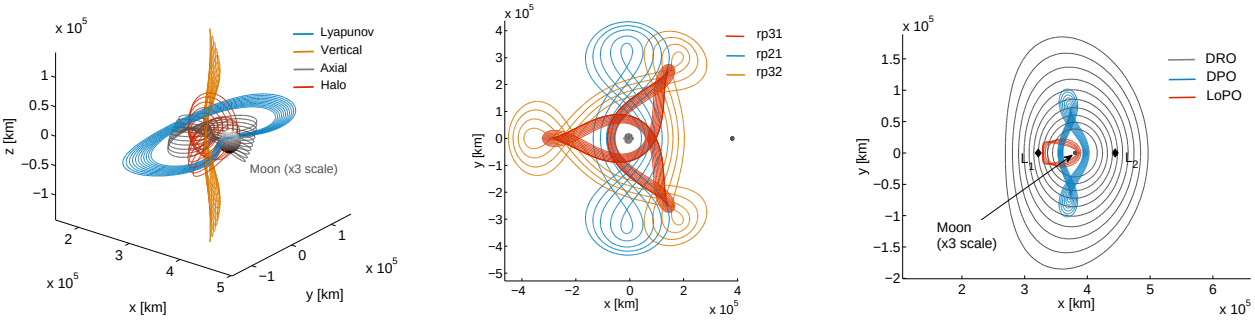

(a) Libration Point Orbits (b) Resonant Orbits (c) Moon-Centered Orbits

Figure 3. Sample members of well-known orbit families in the Earth-Moon system, plotted in the rotating frame.

system and exhibit characteristics consistent with various local dynamical regimes (such as quasi-periodic motions or invariant manifolds). They, therefore, offer several alternatives that have been explored for potential mission concepts. Trajectories in the vicinity of the collinear points are often considered for space infrastructures dedicated to support lunar and solar system exploration;[4,11] orbits in the vicinity of the equilateral points have been recently proposed for the long-term storage of a captured asteroid, partially due to their stability properties.[12] To date, the ARTEMIS mission[6] and specific phases of the Hiten mission[13] have successfully demonstrated the use of libration point orbits and their associated dynamical structures.

Resonant orbits are frequently employed in the design of interplanetary transfers throughout the solar system.[14] Resonant orbits were originally defined as conic arcs within the context of Keplerian dynamics, such that the orbital period of the spacecraft orbit forms an integer ratio with the orbital period of a celestial body. As depicted in Figure 3(b), such solutions can be transitioned to the multi-body regime in the Earth-Moon system, whereas the orbits possess periods that can be approximately described by a rational ratio compared to the lunar orbital period. By convention, a p:q resonant orbit implies that the vehicle accomplishes q revolutions along the reference orbit in the same time interval that the Moon requires to complete p orbits about the Earth. Resonant orbits can offer favorable stability conditions, as the 3:1 resonance that was successfully exploited by the Interstellar Boundary Explorer (IBEX) mission;[15] similar considerations underlie the proposed 2:1 resonant orbit about the Earth, intended for use during a scientific observation phase of the upcoming Transiting Exoplanet Survey Satellite (TESS) mission.[16] Besides stability advantages, resonant orbits may also extend from the Earth vicinity to various, more remote, regions of the Earth-Moon space. There is, therefore, significant interest in exploring resonances as possible transfer mechanism within the Earth-Moon system.[17]

Moon-centered and Earth-centered families include orbits that encircle either the Moon or the Earth, but, in contrast to resonant orbits, their period does not necessarily correlate with the period of the Moon. Also, at this time, Moon-centered and Earth-centered families are typically comprised of low altitude orbits relative to the corresponding central body. Some of the Moon-centered orbits in this investigation are depicted in Figure 3(c). Distant Retrograde Orbits (DROs) and Distant Prograde Orbits (DPOs) have both been recently considered for different applications within the Earth-Moon system. Long-term storage orbits for an asteroid retrieval concept have aroused interest in DROs, mainly because orbits in such a family are predominantly stable and, thus, potentially require little propellant for station keeping.[18] Possible low-cost transfer mechanisms between the L_1 and L_2 Lyapunov orbits as well as lunar parking orbits are, in contrast, mission concepts that could be accomplished leveraging members of the DPO family.[10,19] Similar families also exist in the Earth vicinity, however, note that the only type of Earth-centered orbit utilized thus far in this investigation is LEO. Expansion of the catalog in ongoing, however. To conclude, Table 3 reports a summary of the classes incorporated thus far along with the current applications within the Earth-Moon system.

III.C. Operational Costs

To assess and compare the operational costs to transfer and to maintain orbits within the reference catalog, the periodic orbit insertion and station-keeping costs are estimated. Preliminary estimates of the operational costs may serve to quickly assess some elements of the ΔV budget, potentially influencing other

Table 2. Main categories of families of orbits

Category	Dynamical Origin	Sample Application
Libration Point Orbits	Equilibrium points	Staging and infrastructure placement for solar system exploration missions, scientific observation, lunar surface operations support.[4,11] ARTEMIS mission.[6]
Resonant Orbits	Integer ratio between orbital and Moon's period	Transfer arc, scientific observation. IBEX mission,[15] TESS mission.[16]
Moon-Centered	Moon's dynamical neighborhood	Long-term storage, transfer arc. Asteroid retrieval mission.[18]
Earth-Centered	Earth's dynamical neighborhood	Classical Earth orbit missions.

design trade-offs, such as the choice for the type of propulsion, the mission duration or the spacecraft size and mass. Additionally, the selection of candidate orbits based on the operational costs may not be trivial, as the periodic insertion ΔV and the station keeping manveuvers clash as conflicting objectives. For instance, periodic orbits that possess a manifold structure may allow a low insertion cost through such structures; however, the existence of manifolds implies orbital instability, which may lead to a higher station keeping cost. Low-energy transfers also generally require an extended time of flight, which is undesirable for some applications. It follows that, an interactive trade space may be necessary to compare operational costs across the families included in the reference catalog. Several transfer mechanisms and station keeping strategies are possible; only some representative approaches are currently implemented.

The viability of maintaining each periodic orbit can be measured using a long-term station keeping strategy,[20] which is one representative approach among the many strategies possible. For each orbit, convenient locations for the station keeping maneuver are identified; typically, the x-axis or the xy-plane crossings are selected. In terms of ΔV, the crossings do not generally represent the global minimum cost along the path but they facilitate the practical implementation of the maneuver, whereas the ΔV cost is not excessively higher than the minimum. At the initial location, along the reference path, random normal errors are applied to the state vector. Error distributions in each position component possess a standard deviation of 1 km, while velocity errors are modeled with a standard deviation of 1 cm/s in each direction. Beyond the initial perturbation, the trajectory is integrated forward until the next maneuver location. A locally optimal maneuver is then computed to target the original position of the spacecraft 12 revolutions downstream. Next, the state errors are applied and the maneuver is implemented; the maneuver includes an execution error in the ΔV magnitude, which is assigned using a normal distribution with a standard deviation of 1% relative to the nominal value. The procedure is repeated assuming a fixed final horizon, until 12 revolutions have been accomplished. The final total cost is the sum of the magnitudes corresponding to each maneuver along the trajectory. For each orbit, a Monte Carlo simulation including 500 trials is completed and the average of the total $|\Delta V|$ is linearly extrapolated to produce a representative estimate of the cost that is required to maintain a selected periodic orbit over one year.

As a preliminary exploration of the time of flight (TOF) and the ΔV cost that is required to transfer from a Low Earth Orbit (LEO) to the desired operative orbit, the reference catalog incorporates two common transfer options: a direct path as well as one incorporating a powered lunar flyby. Both types of transfers assume departure from a 300-km altitude LEO as a representative starting orbit. After using the catalog to select candidate orbits that may meet the mission objectives, other types of transfer to the selected orbits may be explored in an advanced trajectory design environment, such as ATD. The concept for the direct transfer, as apparent in Figure 4(a), involves only two impulsive burns: one ΔV_{LEO} to depart the LEO orbit and one ΔV_{POI} to insert onto the final periodic orbit. The powered lunar flyby, Figure 4(b), includes one extra maneuver, ΔV_{Mid}, at a 200-km periapsis distance relative to the Moon, resulting in a 3-burn transfer. To construct the transfer, conic arcs are connected to form an initial guess. These are then corrected with a multiple shooting algorithm in the CR3BP regime. During the corrections process, the following constraints are enforced: departing and arriving locations, LEO inclination relative to the xy plane, tangential burn at LEO, and lunar periapsis (when applicable).[21,22] For transfer to three-dimensional orbits from LEO, note that the LEO inclination is fixed to 28.5° above the Earth equator; however, the inclination of the Earth-

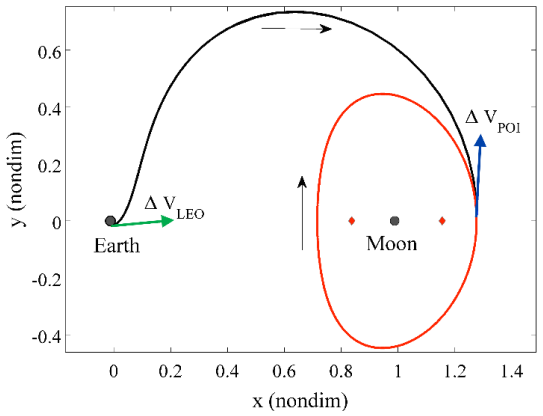

(a) Direct Transfer.

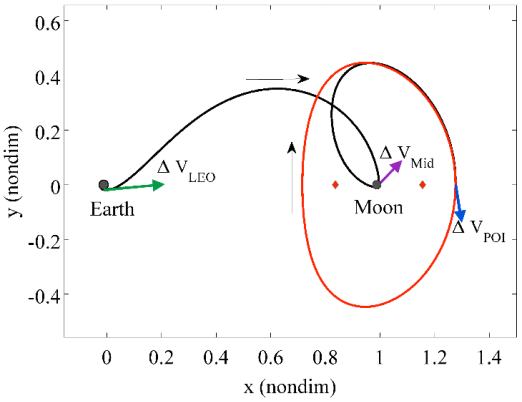

(b) Powered Lunar Flyby.

Figure 4. Sample transfers to periodic orbits within the Earth-Moon system.

Moon orbital plane is known to oscillate between 18.14° and 28.72°. Therefore, the inclination of the LEO with respect to the xy-plane may approximately vary from 0° to 10°. Accordingly, $i_{min} = 2°$, $i_{mean} = 4.99°$, and $i_{max} = 10.37°$ are incorporated to offer reasonable comparisons. For transfer to a planar orbit, only an inclination of zero degrees relative to the Earth-Moon plane is evaluated, for simplicity. Besides the LEO inclination, another distinction for representative transfers, for creating a reference catalog database, involves different insertion locations along the arrival orbit. Next, the trajectory is optimized using a sequential quadratic programming algorithm in MATLAB's fmincon function, subject to the described constraints. The optimization process minimizes $|\Delta V_{POI}|$ for direct transfers and $|\Delta V_{POI}| + |\Delta V_{Mid}|$ for powered lunar flybys. These quantities are selected as most representative of the cost associated with reaching a desired periodic orbit from a low Earth orbit.[21] Of course, multiple-burn transfers and manifold connections could further reduce the local or total ΔV's; nonetheless, the current implementation is adequate to define a set of simplified metrics to trade-off various scenarios. Future developments of the catalog, could incorporate a more complex framework for transfers.

III.D. Simple Statistical Representations

In a design framework for trajectory comparisons, it is essential to create a compact representation of several type of orbits along with their distinctive characteristics. The orbital parameters described in Section III.A, such as the Jacobi constant, the orbital period or the stability index, often evolve along the family in a nonlinear fashion. Thus, it is challenging to simultaneously visualize several characteristic curves. Summary information may be developed in the form of a mean, range and standard deviation representing a desired quantity along a given family. More complex statistical figures may later be introduced. A list of selected orbital parameters is summarized in Table 3; the table includes the current set of families available in the catalog, which are labelled consistent with the legend in Figure 5. However, no immediate comparison is evident from a list format, such as in Table 3. A clearer portrait may emerge from a visual representation.

The first simple visual description employed in the catalog is a scatter diagram. For the selected quantity, each family is represented by a single circle located at the mean value, whereas the size of the circle is scaled over the range of the parameter values across the family. For instance, in Figure 6 this format is adopted to compare the stability index between several families (recall the legend in Figure 5). A small circle located near a unitary value of stability index depicts a family that is comprised of orbits with a significant range of stable members. Thus, it may preliminarily indicate orbits that are surrounded by bounded quasi-periodic motion. Conversely, a large circle located at a relatively large value of the mean stability index describes a family that, not only certainly possesses unstable members, but is also comprised of a large span of orbits at different instability levels. Such an observation may be useful during the search for unstable periodic orbits that may offer a transfer mechanism to access various regions of the Earth-Moon space.

An alternative visual description to compare families of orbits is a bar diagram. In this representation, the range in the values of a certain quantity across each family is described by a bar, with the lower and upper bounds highlighted by horizontal lines. For instance, the range of Jacobi constant values is compared in Figure 7, reflecting the energy levels of the families currently present in the catalog relative to each other.

Table 3. Main statistics for families of orbits within the Earth-Moon system to date (statistics are based on the range of orbits currently available for each family).

Family	JC [ndim]			Period [days]			stab. index [ndim]		
	min	max	mean	min	max	mean	min	max	mean
A1	2.9918	3.0214	3.0064	17.15	17.65	17.40	2.0034e+02	2.5423e+02	2.2729e+02
A2	2.9671	3.0138	2.9916	18.72	19.20	18.94	1.2788e+02	1.6766e+02	1.4713e+02
A3	0.0165	1.8588	0.8147	27.19	27.21	27.20	1.0499e+00	1.1607e+00	1.1245e+00
DPO	2.9941	3.1827	3.1150	5.82	28.00	13.10	1.0000e+00	1.3428e+03	3.0243e+02
DRO	1.4352	3.0180	2.1184	5.87	27.38	24.63	1.0000e+00	1.0002e+00	1.0001e+00
H1	-1.0159	3.1743	1.6171	7.83	13.56	12.30	1.0000e+00	1.1805e+03	1.6618e+02
H2	3.0152	3.1519	3.0649	4.00	14.83	10.56	1.0000e+00	6.0392e+02	1.1281e+02
H3	1.0519	2.4221	1.6759	22.57	27.09	26.64	1.0000e+00	1.3825e+00	1.2081e+00
LP4	2.2710	2.9979	2.7789	91.49	113.86	107.02	1.0000e+00	6.1826e+01	2.0877e+01
LP5	2.2710	2.9979	2.7789	91.49	113.86	107.02	1.0000e+00	6.1826e+01	2.0877e+01
LoPO	3.1805	3.5268	3.2230	0.86	11.50	6.74	1.0000e+00	2.4865e+01	3.9653e+00
Ly1	2.1242	3.1741	2.6482	11.91	32.35	27.93	5.3668e+01	1.1777e+03	2.3196e+02
Ly2	2.9800	3.1702	3.0619	14.66	21.65	17.39	8.0928e+01	7.1415e+02	2.8549e+02
Ly3	1.4601	3.0120	2.0721	27.00	27.28	27.16	1.0000e+00	1.6765e+00	1.2176e+00
rp11	1.3683	3.4794	2.0674	0.77	27.39	24.17	1.0000e+00	1.0002e+00	1.0001e+00
rp12	1.0922	2.7982	1.7497	48.57	54.65	53.94	1.0000e+00	2.1245e+01	2.2720e+00
rp13	0.8915	2.8388	1.9324	71.99	81.93	79.36	1.7266e+00	5.2358e+02	5.7060e+01
rp21	1.8348	21.1473	4.9479	0.29	27.43	18.62	1.0000e+00	1.0000e+00	1.0000e+00
rp23	1.4064	2.9760	2.3060	71.67	81.87	78.48	1.0001e+00	9.5702e+01	1.9882e+01
rp31	2.1801	3.2213	2.8358	27.17	27.38	27.28	1.0000e+00	1.0000e+00	1.0000e+00
rp32	2.7058	3.0583	2.9186	45.77	56.49	52.61	1.0000e+00	5.3221e+01	1.7760e+01
rp34	2.1438	3.0509	2.7117	72.37	110.95	101.36	1.0000e+00	2.2464e+03	6.6119e+02
rs11	1.8485	2.3688	2.1102	27.10	27.34	27.25	1.0000e+00	1.0000e+00	1.0000e+00
rs12	-1.0809	2.8043	0.6243	48.79	54.87	54.26	1.0000e+00	2.0042e+01	5.1336e+00
rs13	-1.1230	2.7216	0.8100	78.00	82.11	81.41	1.0000e+00	3.1175e+01	7.6453e+00
rs21	2.0835	2.7589	2.4614	27.24	27.25	27.24	1.0000e+00	1.0000e+00	1.0000e+00
rs23	-1.2503	2.8650	0.5391	73.55	82.38	81.16	1.0000e+00	8.5749e+01	2.1451e+01
rs23B	1.1932	2.0433	1.6533	81.58	81.72	81.66	1.0000e+00	1.3804e+00	1.0670e+00
rs31	2.1175	3.1850	2.6777	27.17	27.19	27.18	1.0000e+00	1.0000e+00	1.0000e+00
rs32	2.9190	3.1479	2.9952	39.23	50.87	42.49	1.0000e+00	1.7916e+03	4.3464e+02
rs34	2.6231	2.9440	2.8563	79.09	104.59	93.09	2.8774e+01	1.6271e+07	9.7352e+05
SP45	1.7922	2.9880	2.4664	27.20	28.58	27.74	1.0000e+00	1.0000e+00	1.0000e+00
V1	-0.8364	3.1883	1.3843	12.03	27.36	24.20	1.0001e+00	1.6796e+03	2.5191e+02
V2	-1.1263	2.9674	0.7484	19.20	27.34	26.53	1.0057e+00	2.4175e+02	1.0439e+02
V3	-1.3286	2.5831	0.4936	27.14	30.25	27.53	1.0000e+00	1.5964e+00	1.2203e+00
V45	-0.6435	2.9846	1.1676	27.28	27.40	27.36	1.0000e+00	1.0049e+00	1.0022e+00
HS	1.9102	3.0121	2.8153	173.80	231.39	199.61	1.0000e+00	1.9154e+05	4.0898e+04

Any bars that overlap vertically indicate that some members from each family exist at similar energy levels. Such an observation may underlie the rapid selection of candidate orbit families that may be connected by low-cost links. In fact, two periodic orbits at comparable energy levels may be linked by low-cost transfers.[10] Even though a more extensive investigation of low-cost transfers would be warranted, the quick identification

of candidates satisfying a particular mission objective can be a desired feature in the early design phase.

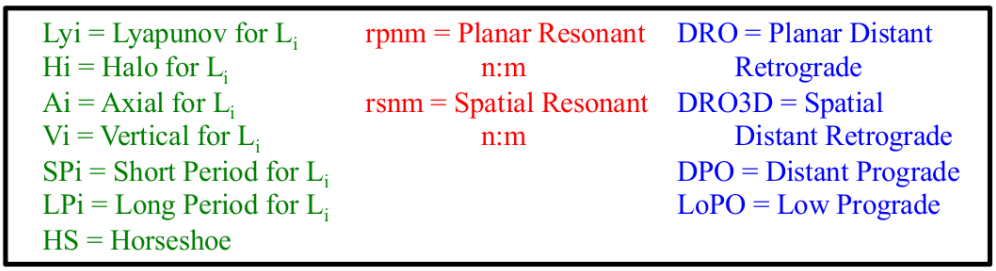

Figure 5. Legend of abbreviations, colored by class.

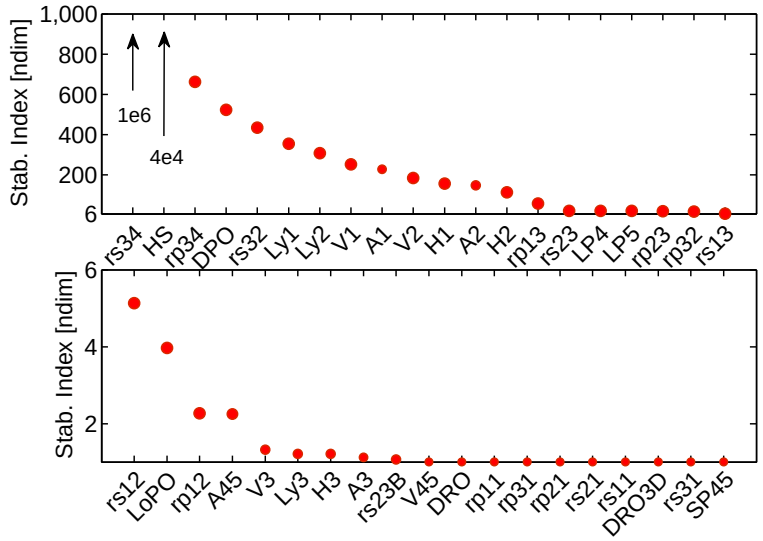

Figure 6. Sample dot representation of stability index of all families available in the reference catalog.

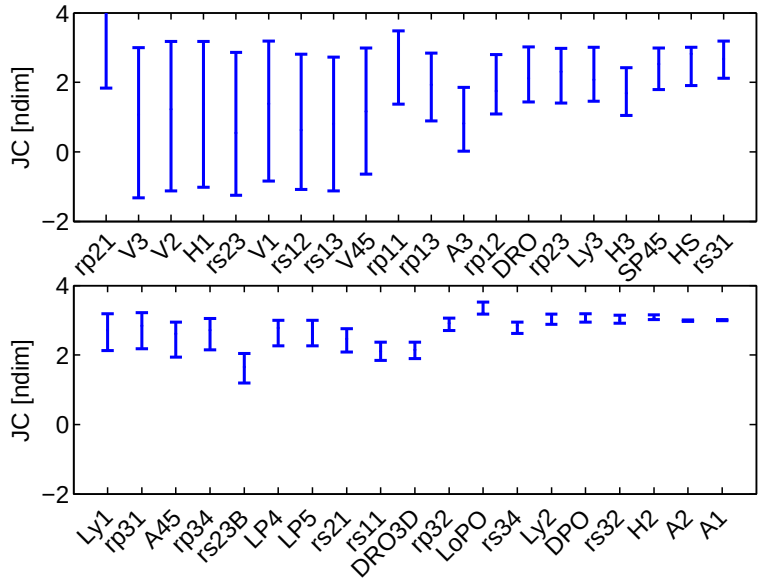

Figure 7. Sample bar representation of Jacobi constant over all families available in the reference catalog.

IV. Dynamic Catalog Implementation

The basic framework for efficient trajectory comparison and design from Section III, is practically implemented in a prototype interactive interface. The form of a Graphical User Interface (GUI) best fits the concept of a dynamic catalog, as it allows easy and immediate data manipulation and visualization. For this investigation, the GUI prototype is developed using the MATLAB® environment. The catalog GUI stands alone or can be incorporated as a pre-processing step in a more extensive trajectory design tool, such as GMAT.[8] For demonstration it is incorporated into the Adaptive Trajectory Design (ATD) software,[10] developed at Purdue University. After the framework is developed, it can also be adapted to a web-based interface. The main features of the new catalog interface include different strategies for orbit selection, access to the orbital parameters and operations costs (in the form of both simple statistics and characteristic curves), data filtering, interactive data visualization, different charts for trajectory trade-offs, as well as guidance for users less familiar with the dynamical structure of the Earth-Moon system. It is assumed that the ultimate capability is the selection of a range of orbits that can be stored and exported for later examination in a trajectory refinement tool such as ATD. A general overview of the design process adopting the ATD-embedded dynamic catalog is summarized as follows:

1. Run stand-alone version or call the catalog interface within an advanced trajectory design environment
2. Select the orbit selection strategy
3. Examine and select families according to the preferred strategy
4. Examine and filter orbits of the selected families
5. Select and store range of orbits within the selected families
6. Import selection to an advanced trajectory design environment for the end-to-end trajectory construction and correction process

From the above list, points 2-4 specifically describe the rapid trajectory assessment and selection procedure. For clarity, the general flow of this process is summarized in Figure 8. To initiate the quick assessment strategy, the flowchart in Figure 8 offers two strategies that are available to search the candidate families for trajectories likely to meet a set of mission objectives or constraints. Each strategy involves different selection criteria: the first strategy, identified as *Categories*, bases the selection on the classification of periodic orbits as discussed in Section III.B; in the second *Global Portrait* strategy the selection is evaluated through a global overview of the orbital parameters across different families (in the form of the simple statistical representations from Section III.D), regardless of their denomination. These approaches are not exclusive and the trade-off process can be accomplished alternating between the two strategies. At the next level, the user gains access to more detailed information on the selected families, such as the complete characteristics curve; hence, the interface enables the selection of a range of orbits, within the family, that best fits into the design requirements. Filtering tools are also available at this level to assist the user. Once suitable sets of periodic orbits are identified, the selections are stored to be plotted in configuration space, to create summary tables of their characteristic quantities, or to be exported to ATD or other design algorithms.

IV.A. Orbit Selection in a Dynamic Catalog

To demonstrate the utility of the catalog within a trajectory design environment, a prototype embedded within ATD is employed. This demonstration follows the steps of the design process outlined in the previous section and it is illustrated by sequential screenshots.

Access the reference catalog. For this example, assume that a user seeks to rapidly produce potential baseline trajectories for a mission concept within the Earth-Moon system, for which no precomputed trajectories are available. In the absence of an initial guess trajectory, the use of advanced trajectory design packages with high fidelity gravitational models may be difficult and cumbersome. The availability of a "dynamic" catalog within an advanced trajectory design environment may allow the user to explore the design space rapidly and intuitively to conduct trade-offs and facilitate the construction of an initial guess.

Orbit selection strategy. When the catalog opens, the graphical interface may appear as in Figure 9. First, the user may select a predetermined orbit selection strategy. Two strategies are offered and the choice is not definitive: the user can iterate the process using the alternative strategy to identify all the possible

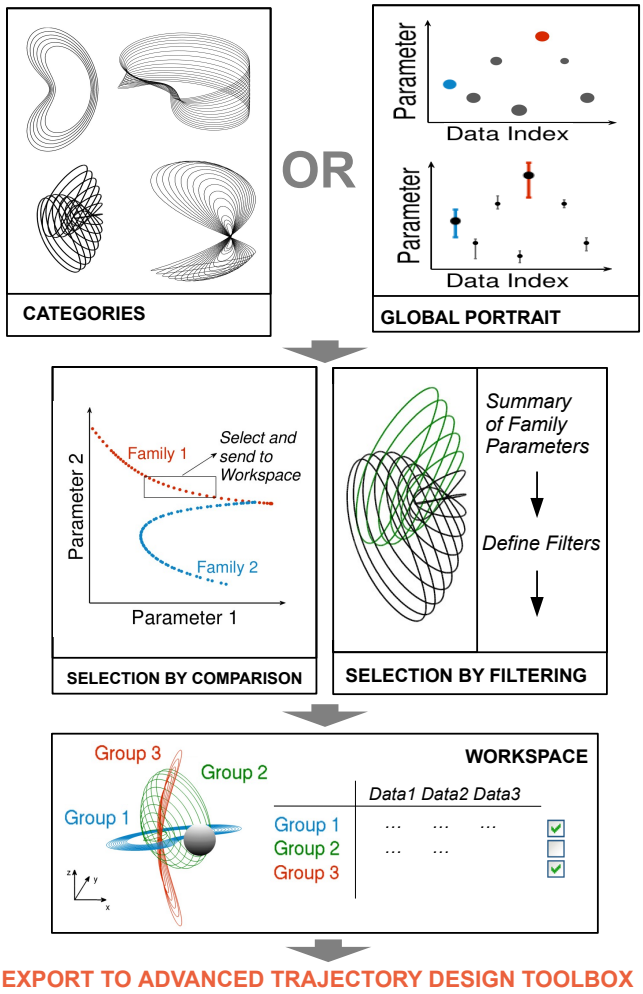

Figure 8. Flowchart representation of the trajectory comparison and selection process.

orbit candidates. The first approach is the selection via *Categories*, which is based on the classification of periodic orbits into classes and families. This strategy may be desired if the user seeks to explore a specific type of orbit (as a result of a literature review or some a-priori knowledge). This selection strategy may also guide the user's understanding of the dynamical structures of the Earth-Moon system. An alternative approach involves selection via a *Global Portrait*, constructed using a simple statistical representation of the orbital parameters across several families. This strategy may be more convenient for a user requiring a preliminary comparison of the orbit characteristics to evaluate the satisfaction of some mission requirements.

Selection via Categories. Figure 10(a) depicts the possible layout of a GUI to facilitate the selection via *Categories*. The orbit classes are represented in the configuration space where sample members of each class are plotted in the rotating frame. On this screen, the user may point and click one of the displayed orbits to choose the desired orbit class. By selecting the desired class the interface updates as displayed in Figure 10(b): in the left-side panel, sample members of various families are displayed to guide the user; in the right-side panel, families belonging to the selected class are listed. The user may then click on members of the list to highlight the desired orbit families and confirm the selection to store the candidate families.

Selection via Global Portrait. Displayed in Figure 11(a) is the possible layout of a graphical interface to aid selection via *Global Portrait*. The left-side of the layout is designed to visually display the orbit data, while controls are located on the right-side of the interface. The top radio-button controls allow the user to switch the form of the composite representation of periodic orbit families from a scatter chart (Figure 11(c)) to a bar chart (Figure 11(a)), and vice-versa. These representations are described in more details

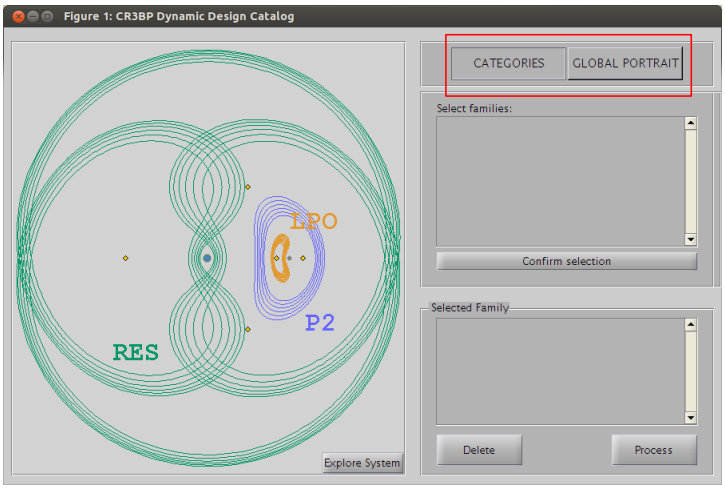

Figure 9. Main panel of the graphical interface for the dynamic catalog. The *red box* highlights the possibility to choose between two different orbit selection approaches.

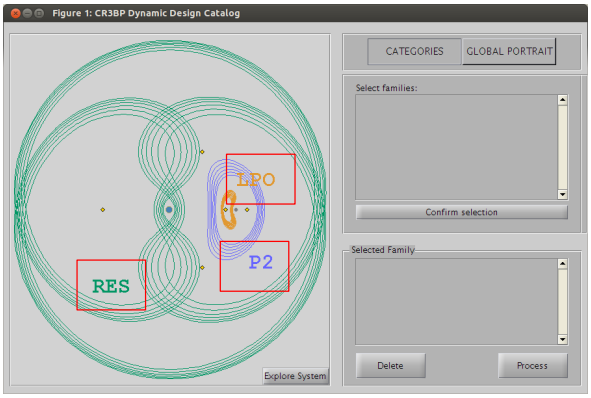

(a) The *red box* highlights the class of periodic orbits: Libation Point Orbits (LPO), Moon-Centered Orbits (P2), Resonant Orbits (RES).

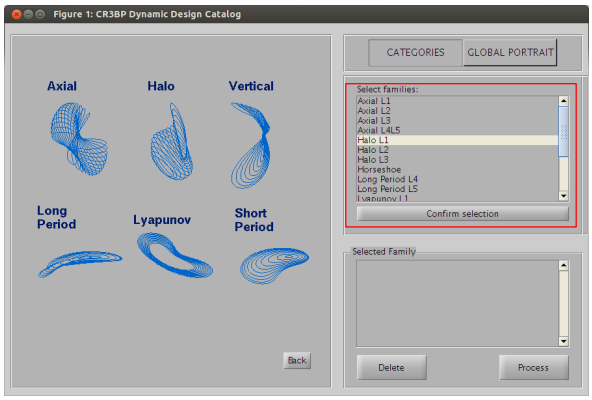

(b) The *red box* highlights the list of families of orbits that belong to the selected class.

Figure 10. Graphical interface to select families of periodic orbits from their classification.

in Section III.D. To manage the set of orbits for the analysis, filtering controls are implemented. This capability currently filters families by class and/or by geometry, but could be easily extended to employ an alternative user-defined criteria. As displayed in Figure 11(b), a new set of families of orbits can be added to the representation. The new set is identified by a different color. By default, each family visualized in the scatter plot is sorted by the mean value of the selected quantity in descending order. Similarly, the data visualized in the bar plot are first illustrated in descending order according to the range size of the selected quantity. The user may modify the characteristic quantities displayed on both axes at any time, and two orbital parameters can be simultaneously examined, as in Figure 11(c). To store families of periodic orbits for further examination, the user can place the pointer over the dots or bars to reveal the name of the corresponding family. The user may then left-click to confirm the selection.

Explore the Earth-Moon dynamical structure. During either selection strategy, the user may gain familiarity with conventional quantities or reference values for the orbital parameters within the CR3BP model. To guide the user, an interactive description of the currently known dynamical structure in the Earth-Moon system is displayed as in Figure 12. On this screen, a control panel displays the principal dynamical regions of interest in the selected three-body system. The user can shift the cursor to the marked area to explore the corresponding region, with reference values for the selected dynamical neighbourhood displayed on the

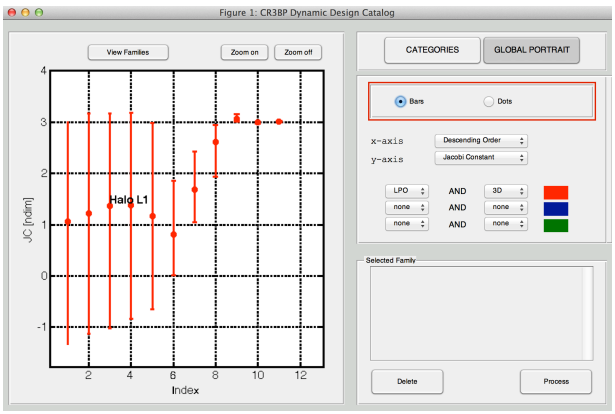

(a) The *red box* highlights the possibility to switch between two simple statistical representations.

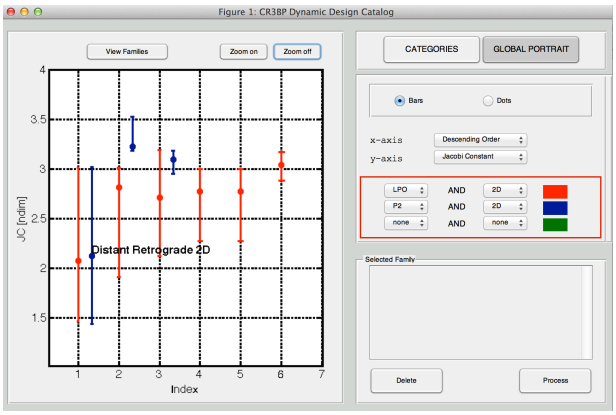

(b) The *red box* highlights the option to filter the current dataset of displayed families or add a new one.

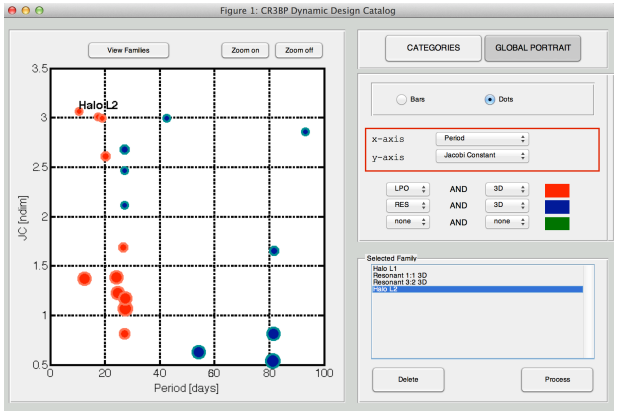

(c) The *red box* highlights the control to modify the characteristic quantities on each axis.

Figure 11. Graphical interface to select families of periodic orbits from a simple statistical representation of their orbital parameters.

screen. Additionally, information about the families in the region is offered: sample members of various families are plotted in the rotating frame, while the mean and range of the orbital parameters across each family are displayed in a table. Several sample families are accessible to the user by scrolling the mouse, while the pointer is over the marked area.

Examine and filter orbits in the selected families. The previous steps yield a set of families that may be good candidate orbits for the mission concept. Next, the selected families are more extensively compared in a two-parameter space. The visualization of two quantities along each orbit is realized using a simple box representation, as demonstrated in Figure 13(a). Analogous to the scatter plot, the location of the box center along each axis is determined by the mean value of the corresponding characteristic quantity; each box is sized using the standard deviation in the corresponding direction. Although the boxes do not precisely reflect the entire characteristic curve along each family, they enable a clear and simple visualization. To view more information about the family, the user is offered the option to show (or hide) the corresponding characteristic curve by right-clicking on the corresponding box and selecting the proper entry from the drop-down menu (see Figure 13(b)). This capability demonstrates the benefit of the inherent interactivity of a catalog of reference solutions. Adding to the interactive features, the user can select the parameter represented by each axis; the currently available options include characteristic quantities describing the orbits along the family as well as the operational costs, such as the ΔV for station keeping maneuvers or the cost of different types of transfers. Moreover, lower and upper bounds, e.g., those that correspond to some mission requirements, can be applied to each orbital parameter. As illustrated in Figure 13(c), orbits that do not satisfy the filtering criteria are removed from the characteristic curves. The result of this stage of the orbit selection process is the identification of the ranges of orbits across several families that may likely fulfill the mission objectives.

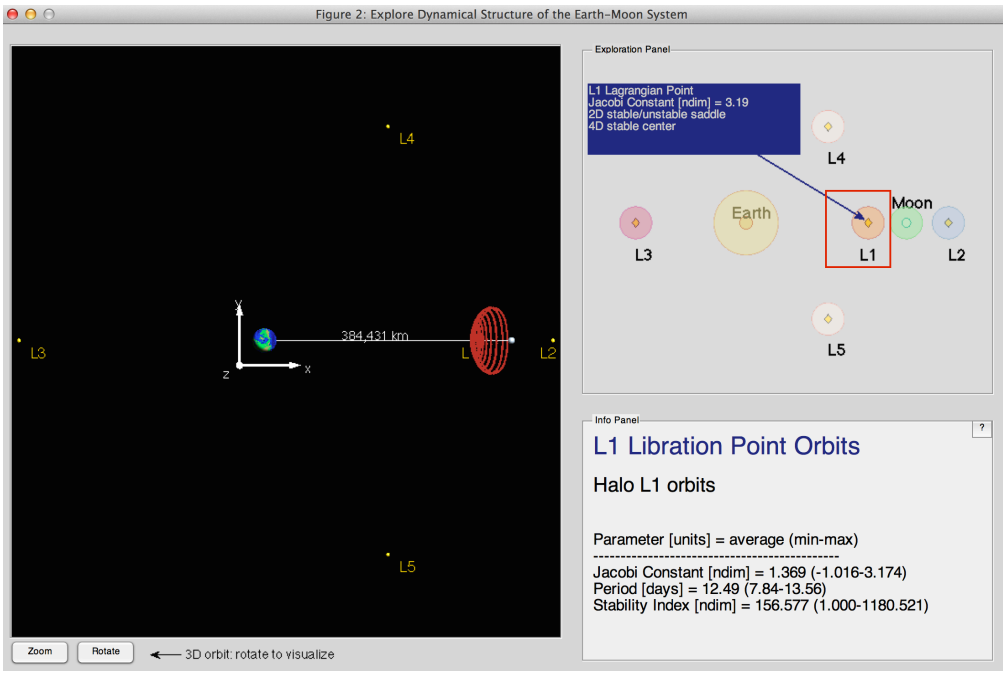

Figure 12. Interactive description of the dynamical structure of the Earth-Moon system. The *red box* highlights the cursor hovering over a marked area in the control panel. Reference values for the selected dynamical region are displayed in the dark-blue box. The sample family is plotted into the rotating frame on the left, whereas the corresponding orbital parameter statistic are in bottom-left panel.

Select and store a range of orbits within the selected families. Once the user has completed the exploration of the possible trade-offs, specific members of each family are selected by right-clicking and choosing the appropriate item for the drop-down menu. The selected orbits are plotted in black on the characteristic curve, as seen in Figure 14(a). The operation can be repeated to include orbits belonging to different families. After the selection is completed, it can be saved to a workspace using the drop-down menu that appears on the right-click of the mouse. Selections stored in the workspace can be visualized in the configuration space (Figure 14(b)), a summary of their orbital parameters can be written in a text file, or can be exported into ATD.

Import candidate orbits into an advanced trajectory design environment for the end-to-end trajectory construction. After a set of periodic orbits is exported from the catalog interface, they are loaded directly into the list of available orbits, e.g., into ATD, as demonstrated in Figure 15(a). If straightforward transfers are available for the selected family members, the user is offered the option to also import the transfer trajectory into ATD. Any trajectory exported can be incorporated into an end-to-end mission baseline using the standard capabilities of ATD. Ultimately, using the ATD graphical interface depicted in Figure 15(b), the trajectory constructed can be propagated and corrected in either the CR3BP or ephemeris model. Several type of mission constraints can also be incorporated in the correction process. Alternatively, catalog data can flow directly into GMAT.

V. Application to Trajectory Design in the Earth-Moon System

To demonstrate the use of this framework for an interactive reference catalog of solutions, two mission design applications are discussed. The first example concerns long-term storage options near the Moon, while the second example involves the orbit selection for astrophysical observatory missions, based on the IBEX and TESS missions concepts.

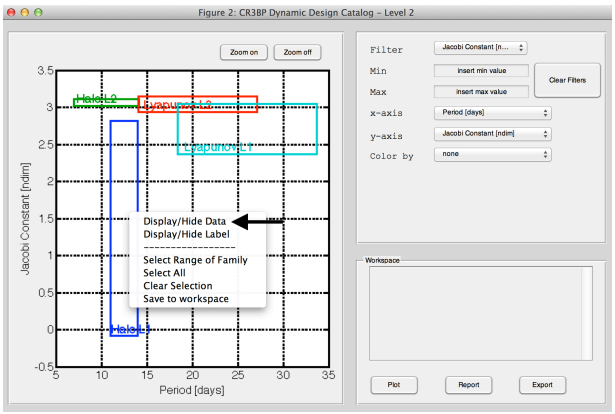

(a) The *black arrow* indicates the item of the drop-down menu to show/hide the characteristic curve.

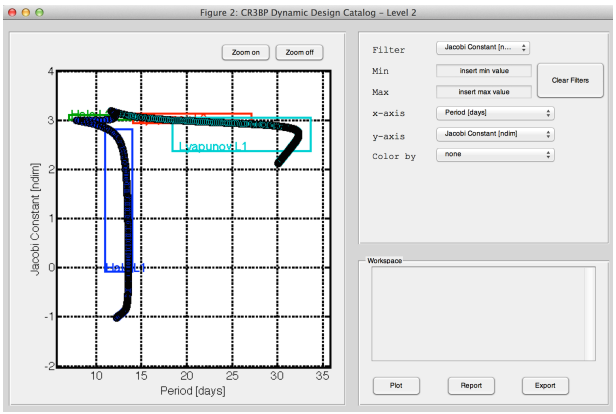

(b) Characteristic curves are displayed for selected families.

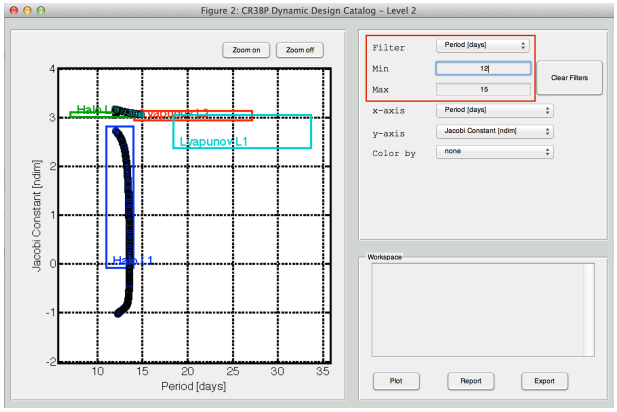

(c) The *red box* in right panel highlights the controls to set lower and upper bounds on the orbital parameters. Orbits outside the bounds are removed from the plot.

Figure 13. Graphical interface to compare family of periodic orbits in a two-parameter space. A simple box representation is adopted. Characteristic curves can be optionally displayed. Filter can be applied to the dataset.

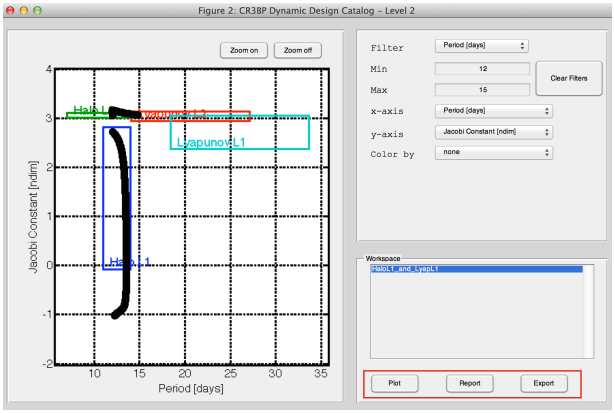

(a) The *red box* highlights the options to process the selection of periodic orbits stored in the workspace.

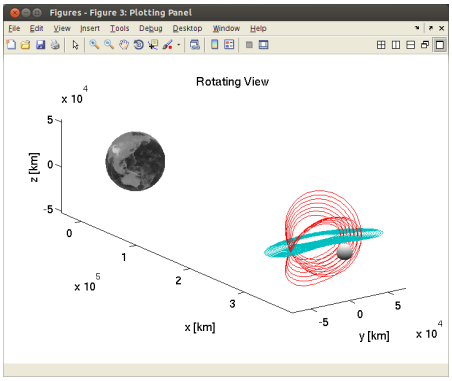

(b) Selection from the workspace is visualized in the Earth-moon rotating frame (Earth and Moon size is magnified).

Figure 14. Periodic orbits are colored in black when selected (a). The current selection can be stored in the workspace to be plotted in the configuration (b) space or exported to ATD.

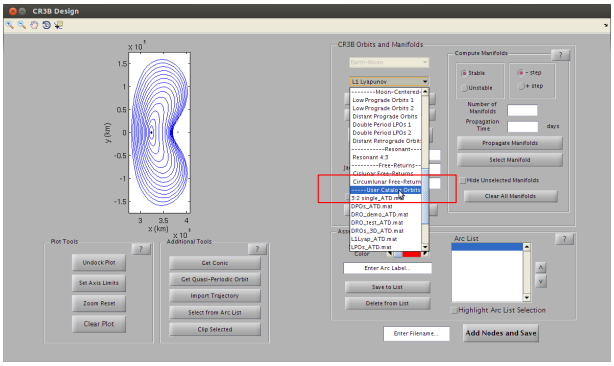

(a) The *red box* highlights the orbits exported from the interactive catalog, automatically loading into ATD.

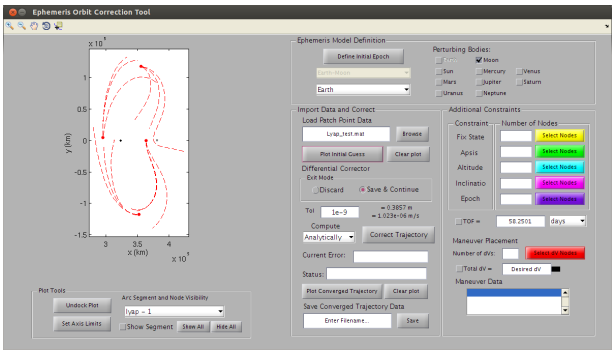

(b) Graphical interface for trajectory correction in ephemeris model.

Figure 15. Graphical interfaces of the ATD software for end-to-end trajectories design in a multi-body regime.

V.A. Long-term Space-based Infrastructure

Long-term space-based infrastructures in the vicinity of the Moon are a recent concept of interest. Similar facilities may support lunar activities, serve as staging platforms for further exploration of the solar system, supply human habitats or offer storage locations for retrieved asteroids. To select a candidate orbit for the sample scenario enabling long-term storage of space-based infrastructure, a list of potential mission requirements is first defined:

- *The storage orbit should enable lunar surface operations.* To facilitate communications with the lunar surface or to commute material and personnel between facilities on the lunar surface and the home base, the orbit should be reasonably close to the Moon.

- *Orbit must be maintained for at least several years.* Over long intervals of time, station keeping and orbit determination may be challenging in a multi-body environment. Accordingly, the orbit should have a low stability index, indicating a lower sensitivity to external perturbations. Behavior of vehicles in such orbits may be easier to predict and maintain.

- *Accessible from L_1 or L_2 Lyapunov orbits.* L_1 or L_2 Lyapunov orbits may be used for staging and manifold transfers. Accordingly, the value of the Jacobi constant of the candidate orbit should be close to the Jacobi constant of orbits in the L_1 and L_2 Lyapunov families, indicating the potential low-cost for transfers to those orbits.

- *Accessible from LEO without excessive limitations.* The transfer from LEO to a candidate orbit should have a low ΔV budget and the orbit period should not heavily restrict on-orbit rendezvous opportunities.

These requirements may serve as a guide in the early identification of a baseline solution. Although the orbit selection process is inherently iterative, it is demonstrated by a series of common steps.

Step 1. Assuming no prior insight into this dynamical regime, it is reasonable to begin by exploring the dynamical structure in the Earth-Moon system. Using the appropriate catalog interface, note the regions, such as the L_4 vicinity displayed in Figure 16, whose dynamics yield trajectories that are likely to successfully support lunar activities. At first glance, the resonant type orbits and the families associated to the L_3, L_4 and L_5 points are excluded, as their geometry may limit the accessibility and utilization of any infrastructure in vicinity of the Moon. Plotting each family in configuration space reveals, however, that the axial family of periodic orbits near L_4/L_5 extends towards the vicinity of the Moon. Therefore, all the periodic orbits linked to the L_4/L_5 dynamical regime are discarded except for the L_4/L_5 axial family. Also, note that resonant orbits, which are currently excluded as candidate families, may be exploited as transfer mechanisms to a space facility during later stages of the design.[17]

Step 2. The catalog interface for exploring the system dynamics provides additional insight, such as the ranges of JC, of the L_1 and L_2 Lyapunov orbits: $JC \approx [3.188, 2.124]$ and $JC \approx [3.172, 2.881]$, respectively. To facilitate a low-cost transfer to the vicinity of L_1/L_2, candidate storage families of orbits should possess

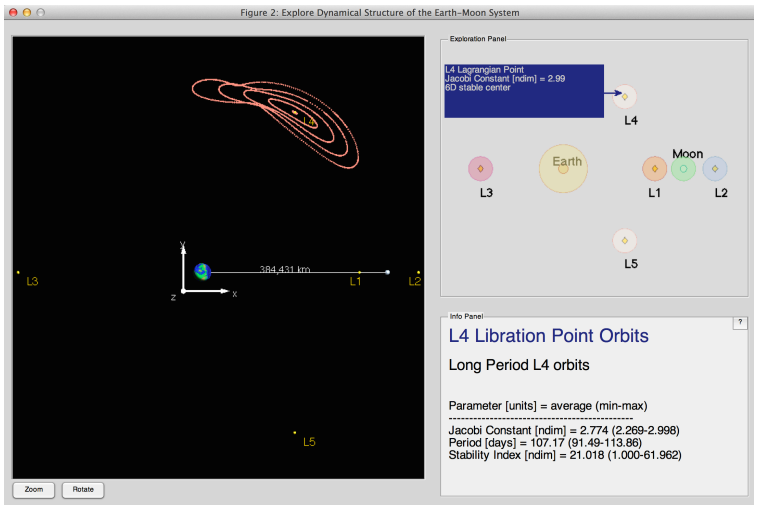

Figure 16. Visualization of the L_4 dynamical region within the catalog graphical interface.

some members with a Jacobi constant that is comparable to the L_1 and L_2 Lyapunov ranges. Thus, the JC ranges for various libration point orbits and Moon-centered families is straightforwardly compared: the interactive catalog interface should appear as in Figure 17, where the bar chart is employed to supply a global portrait. Annotations on this figure correspond to current candidate orbits, for clarity. Referring to the bar diagram in Figure 17, orbits that do not adequately cover the L_1/L_2 Lyapunov JC range, such as LoPOs, the axial L_4/L_5 family or three-dimensional DROs, are excluded from the set of possible candidates. Some orbits, such as the L_1 halo, L_1/L_2 vertical, may almost entirely encompass the reference values of JC, whereas other families of orbits, such as L_1/L_2 axial, may exist completely within the L_1/L_2 Lyapunov energy range. Families that possess some members with a JC comparable to the JC of the L_1/L_2 Lyapunov families include Lyapunov L_1/L_2 (trivially), L_1/L_2 axial, L_1/L_2 halo, L_1/L_2 vertical, distant retrograde and distant prograde periodic orbits, forming a preliminary list of candidates.

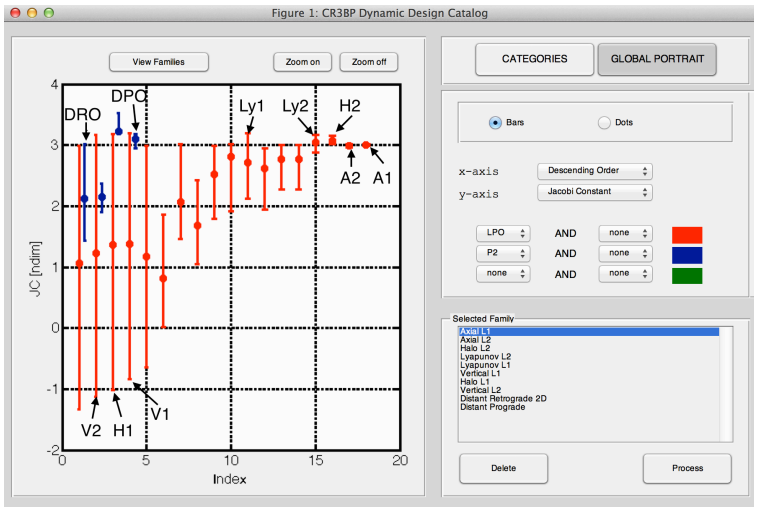

Figure 17. Comparison of JC range across libration point orbits and Moon-Centered families, within the catalog graphical interface. Orbits that satisfy the preliminary JC requirement for a long-term storage mission are labelled (see legend in Figure 5).

Step 3. The mission objectives also require favorable conditions for rendezvous opportunities with a certain space-based infrastructure and long-term maintenance of the storage orbit. Such conditions can be simultaneously evaluated in a two-parameter space, comprised of the orbital period and stability index. A lower orbital period facilitates orbit phasing operations, while a lower stability index value indicates the

potential for long-term stability and predictability of the trajectory. A scatter diagram, depicted in Figure 18, is employed for a concise visualization of the trade space. The radius of each dot is a scaled representation of the range of the orbital period across the family. It seems reasonable to select families with mean period below 20 days and mean stability index no larger the 400. However, these limits are not to be considered absolute criteria, but they are rather "fuzzy" boundaries. Using Figure 18 as a reference, the L_1/L_2 halo and the L_1/L_2 axial families possess a sufficiently low period and stability index. The Lyapunov L_2 family is slightly above the threshold for orbital period, but also possesses large variance for period values, as indicated by the dot size: it is likely that several Lyapunov L_2 orbits have periods lower than 20 days; thus, the family remains viable among the candidates. Although, the mean orbital period across the DRO family is larger than the mean period of other families, its range is quite wide as indicated by a large dot radius. In addition, members of the DRO family possess excellent stability properties (i.e., mean stability index almost equal 1). Accordingly, the DRO family is included among the possible storage orbits. The final list includes: L_1/L_2 halos, L_1/L_2 axials, L_2 Lyapunov, and DRO families.

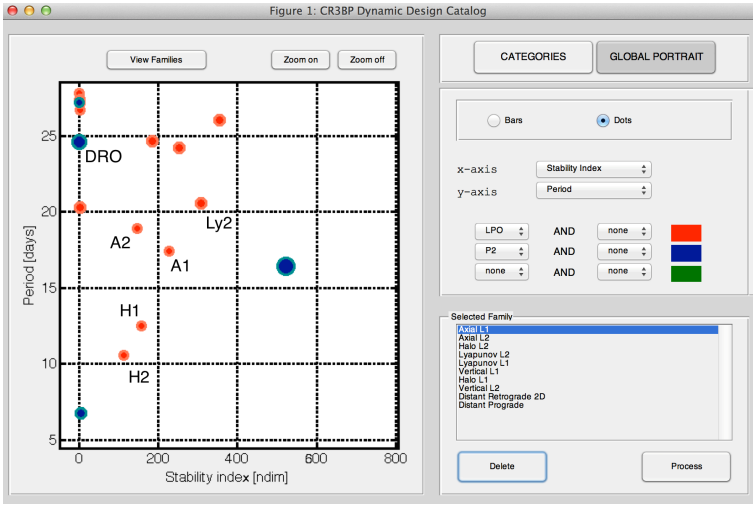

Figure 18. Comparison of the mean values for the orbital period (horizontal axis) and the stability index (vertical axis) across LPO and Moon-centered families, within the catalog graphical interface. Orbits that satisfy the preliminary requirements for a long-term storage mission are labelled (see legend in Figure 5)

Step 4 Next, the operational costs for the current list of candidate orbits are investigated using a simple box representation. Figure 19(a) depicts a box representation of the Periodic Orbit Insertion (POI) cost and annual average station keeping values, that are embedded in a prototype interface of the catalog. Using this figure as a reference, simple direct transfers from LEO to periodic orbit in various families near the second Lagrangian point L_2 have statistically higher periodic orbit insertion costs. Conversely, the DRO and L_1 halo orbits possess, on average, the lowest insertion values, i.e., ΔV_{POI}. In addition, the DRO family also appears to require a small station-keeping budget. While a number of other families included in these operational cost diagrams may possess potential candidates for further analysis, the DROs seem most interesting: they offer favorable geometry with respect to the Moon, low station-keeping costs over nearly the entire range of orbits and low periodic orbit insertion ΔV for a direct transfer from a 300-km LEO. The DRO family is examined further to identify members that could be accessible by a crewed vehicle. Currently, manned mission concepts to complete a roundtrip to the storage location require no more than approximately 21 days, based on restrictions for hardware, supplies, and human factors.[21] This limit of 21 days includes both the outbound and return legs along a transfer arc, as well as the time-on-orbit. Up to one orbital period at the storage location is allowed for on-orbit phasing and rendezvous. Since the time-of-flight to the DRO varies between 5.4 and 7.2 days for both the inbound and outbound leg,[22] the candidate storage orbit must possess an orbital period of, at most, 10 days to accommodate the time required for the transfer legs from and to the Earth. The resulting upper bound on the orbital period is easily evaluated using the on-demand filtering capabilities of the catalog. Interacting with the controls of the graphical interface, a maximum value for the orbital period is set and the trade-off diagram immediately updates: Figure 19(b) shows the diagram before the application of the filter, while Figure 19(c) displays the two-parameter trade space after filtering. The remaining orbits are exported to be employed in a high-fidelity trajectory design environment.

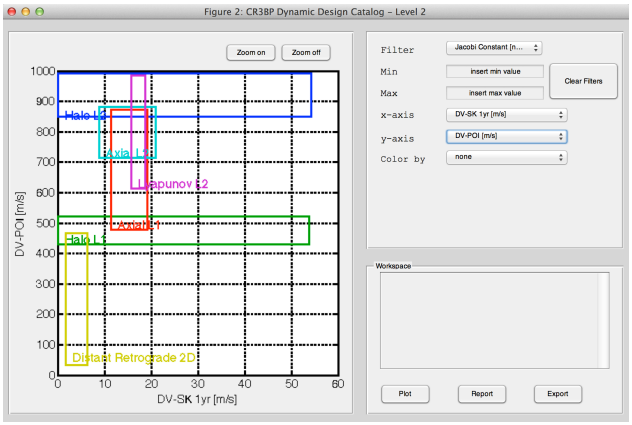

(a) Simple box representation.

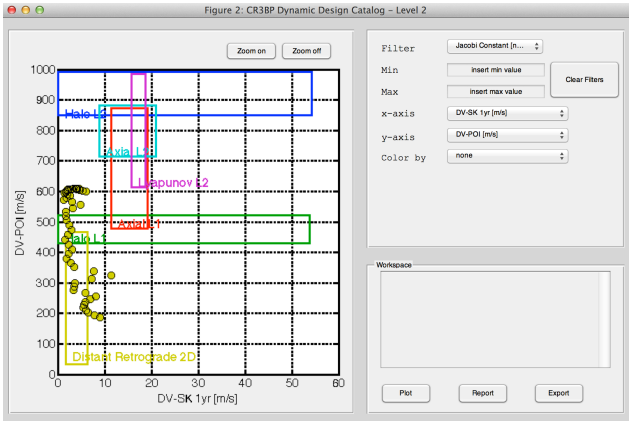

(b) DRO characteristic curve.

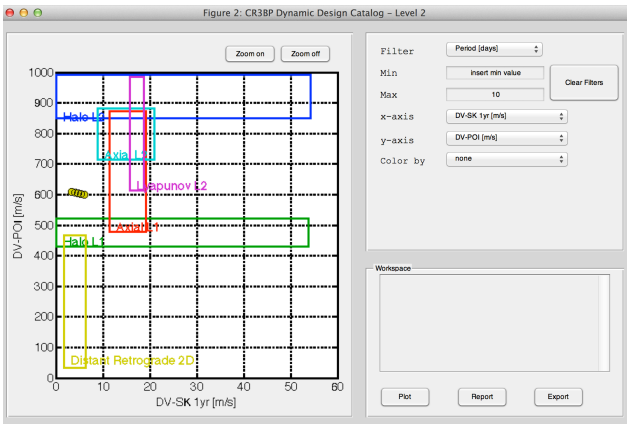

(c) DRO characteristic curve after the application of a maximum orbital period filtering criteria.

Figure 19. Comparison of operational costs (station keeping cost, x-axis; orbit insertion ΔV, y-axis) for candidates orbits for long-term storage facility, within the catalog graphical interface.

Step 5. The rest of this analysis demonstrates that the orbits selected through the interactive catalog can be used in advanced stages of the mission design process. First, the selected range of the DRO family, which is plotted in Figure 20(a), is loaded into a high-fidelity trajectory design environment, such as ATD, and one orbit within the candidate range is selected, possessing an energy-like value $JC = 2.987$ and a period of 7.715 days. The transfer path from LEO to the candidate range of periodic orbits is imported as well. Next, a complete trajectory is constructed in the ephemeris model using the standard ATD capabilities.[10]

The initial guess is displayed in Figure 20(b), including the LEO, the direct transfer from the catalog and multiple revolutions of the periodic orbit. The trajectory is integrated using an ephemeris model that incorporates the gravity of Sun, Earth and Moon. The date of LEO departure is set equal to January 1, 2025 0:00:00 UTC. Two impulsive burns are included: one burn at the departure from LEO and the other maneuver at the insertion into the periodic orbit. An example of a solution converged using the ATD build-in multiple shooting algorithm is displayed in Figure 20(c). The trajectory is plotted in an instantaneously defined rotating, barycentered, Earth-Moon frame. Although a precisely periodic orbit does not exist in the ephemeris model, the corrected transfer and DRO approximately retain the same characteristics as the reference solution that was constructed in the CR3BP. Accordingly, there is significant reduction in computational effort and process simplification in using the catalog of reference solutions in the CR3BP for comparison and identification of periodic solutions that predict some of the dynamical structures that actually persist in an ephemeris model of the Earth-Moon space.

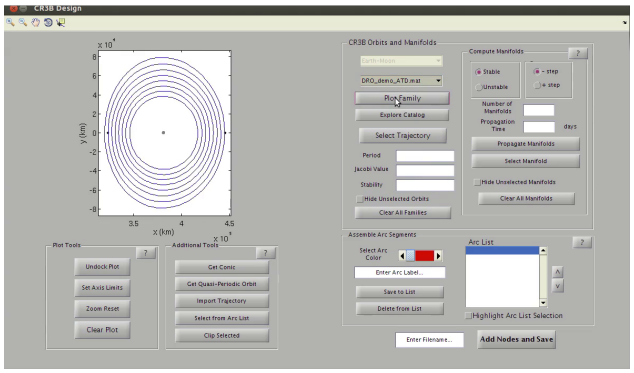

(a) DRO candidate range imported and plotted into ATD.

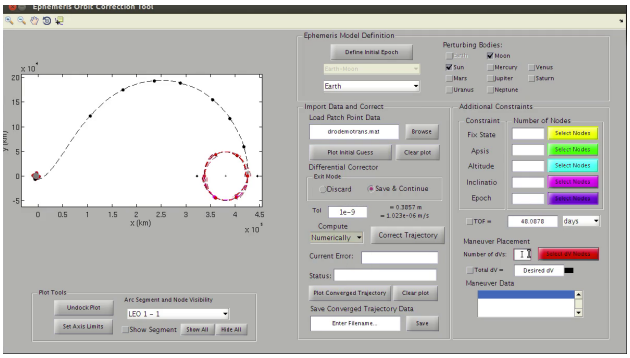

(b) End-to-end trajectory initial guess in ephemeris model.

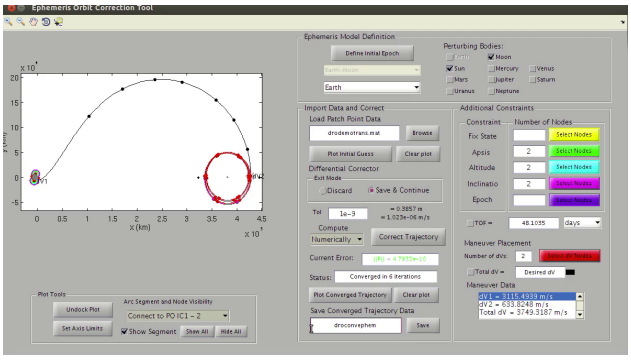

(c) End-to-end converged trajectory in ephemeris model.

Figure 20. Advanced analysis of the selected DRO orbits within ATD.

V.B. Astrophysical Observatory

Recent NASA astrophysical observatories, such as the IBEX or TESS mission concept, have successfully leveraged the multi-body dynamical structure in the Earth-Moon system by exploiting resonant orbits.[15,16] This second example demonstrates the application of the dynamic reference catalog to the preliminary design of a trajectory concept similar to IBEX or TESS mission, which have some common driving requirements, summarized as follows:

- *Facilitate science data collection.* The final orbit should grant an unobstructed view of the sky and allow sufficient time near apogee to collect science data. Raising the apogee radius increases the time the spacecraft spends near apogee. However, increasing the apogee radius weakens the communications signal strength with the ground segment.
- *Robust communications with Earth.* The perigee of the orbit should be close enough to Earth to guarantee high signal/noise ratio of the science data downlink.
- *Lower bound to perigee altitude.* Radiation dose is a serious hazard for many spacecraft components, including delicate payloads. The orbit perigee must be, at minimum, above 2.3 Earth radii to reduce the exposure to the Van Allen radiation belts. Moreover, to minimize the risk of interference or collision with geosynchronous satellites, the perigee should be located beyond the GEO altitude (approximately 35,786 km).
- *Low ΔV budget for orbit insertion.* Both the IBEX and TESS spacecraft possess limited propellant resources. Avoidance of high energetic orbits (low Jacobi constant), since such destination energy levels would likely demand higher ΔV values to acquire the final trajectory. To further reduce the transfer cost, lunar gravity assist may be considered for insertion.
- *Limited time in eclipse.* Power storage capabilities limit the sustainable duration of any eclipse to a few hours.
- *Long term predictability.* The orbit should be characterized by a low sensitivity to external perturbations, as predicted by unitary, or low, stability index. For a trajectory that is well predicted over long time horizons, the eclipse events and the observation schedule can be more accurately determined. In addition, a stable orbit may also include low station keeping costs.

Candidate orbits satisfying these constraints may be selected using the interactive reference catalog. By geometry, the closest approach to the Earth of orbits in the L_1, L_2, L_5 and Moon regions is likely beyond the limit to download the science data. Although some members of these families may satisfy the perigee maximum distance constraint for downlink, a rapid analysis can begin with the examination of dynamical structures that are more likely to guarantee robust science data communications. Resonant orbit and orbits in the vicinity of L_3 exhibit close approaches to the Earth and, therefore, may be considered better candidates. However, L_3 families exist at lower values of the Jacobi constant (higher interval in terms of energy values), possibly requiring an higher ΔV for periodic orbit insertion than for the resonant families. Similarly, resonant families with a low range of values in JC are discarded. Figure 21 displays a bar diagram with JC on the vertical axis and stability index on the horizontal axis embedded within the catalog graphical interface. In Figure 21, the orbits that have an advantageous JC range across the family are boxed. Using this criteria, viable families of resonance orbits include: 1:1 planar, 1:2 planar, 1:3 planar, 2:1 planar and spatial, 2:3 planar, 3:1 planar and spatial, 3:2 planar and spatial, 3:4 planar and spatial.

The families that remains after the previous filters of periodic orbits can be further analyzed, with candidates selected through an examination of the orbital period and the stability index. Although, the spacecraft acquires science data at apogee, the information is not downloaded to a ground segment until perigee. Additionally, it is not possible to lower the apogee to the desirable downlink altitude without compromising the science quality. Therefore, it is reasonable to discard orbits with an excessively long period, to avoid an unnecessary, protracted waiting time between data acquisition and subsequent downlink. Accordingly, the followings resonant orbit families are excluded from the set of candidates: 1:2 planar, 3:2 planar (average period $\approx$ 50 days) and 1:3 planar, 2:3 planar (average period $\approx$ 80 days). Next, resonant orbits that are less accurately predictable over a long-term time horizon, as predicted by a high stability index, are deselected: 3:4 spatial (average stability index $\approx$ 970000), 3:2 spatial (average stability index $\approx$ 500), 3:4 planar (average stability index $\approx$ 660). Both these criteria can be concurrently evaluated in

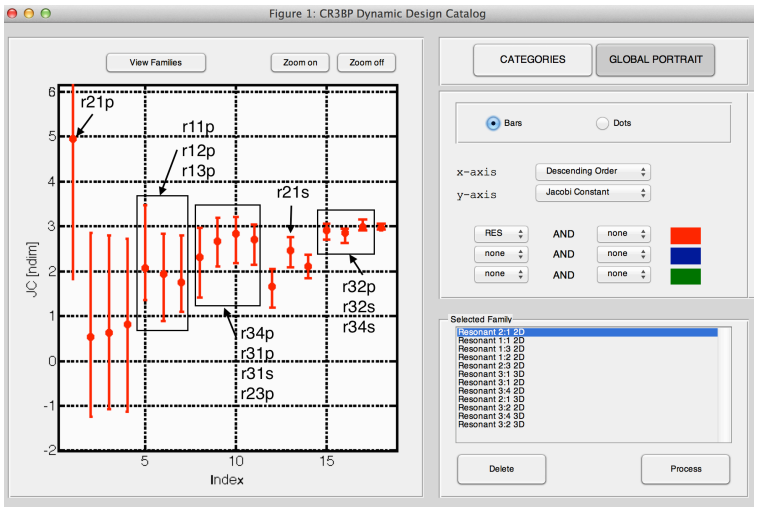

Figure 21. Comparison of JC range across resonant families, within the catalog graphical interface. Orbits that satisfy the preliminary JC requirement for an astrophysical observatory mission are labelled (see legend in Figure 5)

the two-parameter scatter diagram available through the catalog interface, as illustrated in Figure 22. In this figure, the remaining candidate families are indicated by arrows; such candidate families are located in the lower left corner, which represents solutions with statistically low orbital period and low stability index. Further investigation of members of these families reveals satisfaction of the perigee requirements to

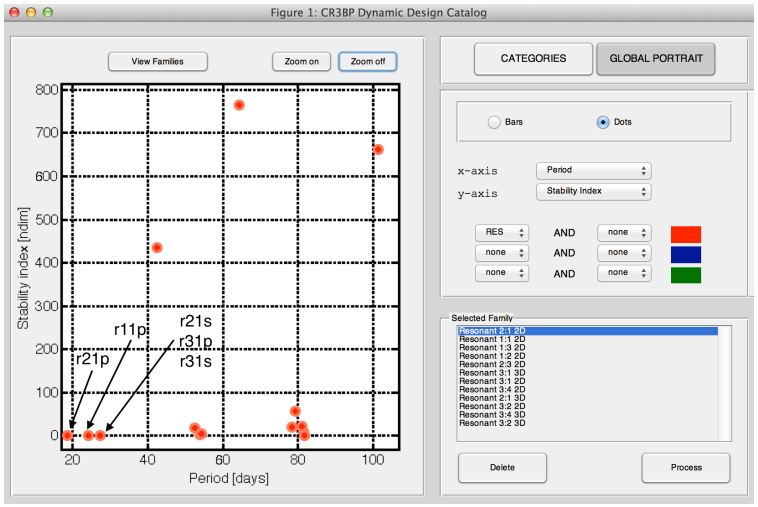

Figure 22. Comparison of orbital period (vertical axis) and stability index mean values (horizontal axis) across resonant families, within the catalog graphical interface. Orbits that satisfy the preliminary requirements for a astrophysical observatory mission are labelled (see legend in Figure 5).

minimize the radiation dose and the collision risk while maintaining effective communications with Earth. Representative bounds on the perigee are adopted from the TESS mission concept: the perigee altitude shall lay between 6 Earth radii ($\approx$ 36000 km) and 22 Earth radii ($\approx$ 132000 km). As depicted in Figure 23, the graphical interface of the catalog guides the rapid selection of orbits that satisfy the set of perigee limitations. In this figure, the characteristic curves are truncated by the 36000-km perigee lower bound and by the 132000-km perigee upper bound using the filtering function. The remaining members possess a suitable geometry, reasonable waiting time between the sky observations and the data downlink, favorable stability conditions, lower energy and they the perigee altitude constraint. These candidate orbits include the 2:1 planar and spatial resonant orbits (plotted in Figure 24(a)), and 3:1 planar and spatial resonant orbits (plotted in 24(b)). It is worth noting that, in fact, the IBEX mission leverages a 3:1 resonant orbit, while the TESS mission incorporates a 2:1 resonant orbit. Throughout this process, 1:1 resonant orbits also emerged as viable candidates and are plotted in Figure 24(c). The results of the rapid mission design process

via the "dynamic" catalog can be transitioned to a higher-fidelity model to complete the design process. As an example, consider a 2:1 resonant orbit with period of 27.25 days and perigees altitude lying at 75,131 km and 70,497 km from the Earth that is imported into ATD. Additionally, the reference catalog includes a representative fly-by transfer in the CR3BP from LEO to the selected orbit that is also exported into ATD (a lunar fly-by may reduce the orbit insertion cost, as desirable to meet the mission requirement for low ΔV budget). The ATD advanced trajectory design environment allows a user to concatenate the 300-km LEO orbit, the transfer arc and multiple revolutions of the selected 2:1 resonant orbit to generate an end-to-end trajectory that is corrected in the ephemeris model. Assuming the epoch equal to August 1, 2045, the 2:1 resonant orbit and the corresponding transfer via lunar gravity assist are displayed in Figure 25, as they appear after the corrections in the ephemeris regime. The periodic insertion cost, which is comprised of $|\Delta V_{POI}| + |\Delta V_{Mid}|$, results in a net value equal to 542 m/s, while the transfer from LEO to the orbit, via the Moon, requires 18.64 days. The trajectory in the ephemeris model retains the general characteristics predicted in the CR3BP using the interactive reference catalog and to meet the sample mission requirements, such as the perigee altitude or the low ΔV budget. Accordingly, there is significant merit in the "dynamic" catalog as a framework for trajectory comparison and selection, rather than directly employing advanced high-fidelity mission support algorithms at the outset. Given the results of the rapid mission design process via the "dynamic" catalog, more advanced trajectory design environments are then effectively applied to further verify that the set of mission requirements are met within the appropriate dynamical model.

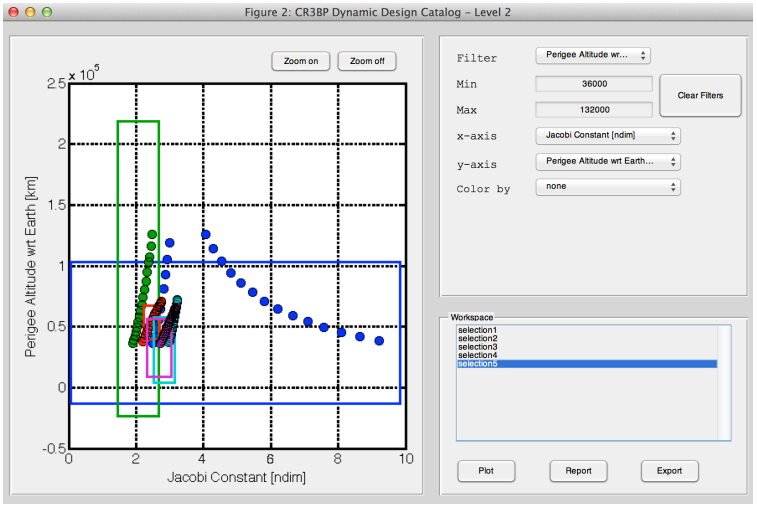

Figure 23. Examination of the perigee altitude of candidate orbits for astrophysical observatory, within the catalog graphical interface. Only orbits that have perigee above 36000 km and below 132000 km are displayed.

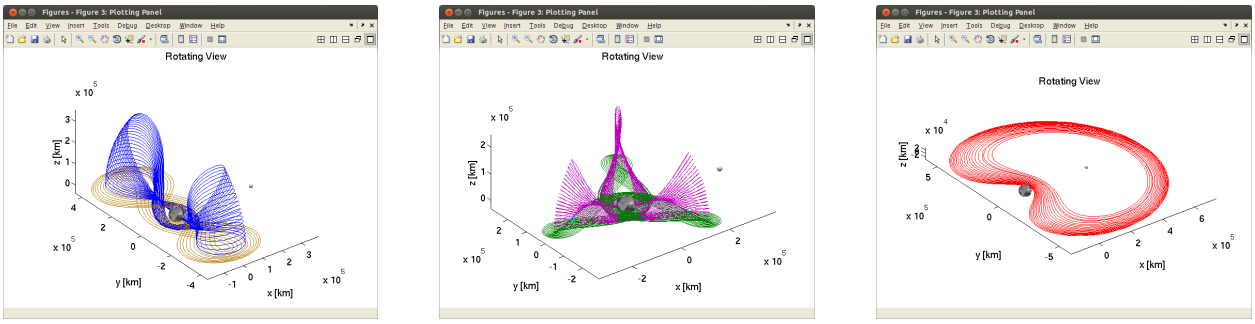

(a) 2:1 resonant planar and spatial selected orbits.

(b) 3:1 resonant planar and spatial selected orbits.

(c) 1:1 resonant planar and spatial selected orbits.

Figure 24. Selected orbits for astrophysical observatory are plotted in the Eart-Moon rotating frame, within the catalog graphical interface.

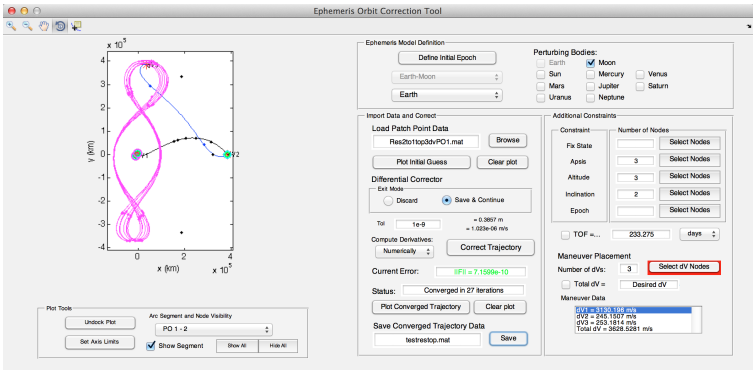

Figure 25. Analysis of the selected 2:1 resonant orbit for astrophisical observatory within ATD: end-to-end converged trajectory in ephemeris model.

VI. Conclusion

In this paper, a framework is constructed for quick and intuitive trade-offs among trajectories that may be used during the preliminary mission design phase. The framework is based on a interactive reference catalog of periodic solutions in the CR3BP, including libration point orbits, resonant and Moon-centered orbits. The current framework enables the inclusion of additional families as new options arise. This dynamic catolog has the capability to compute and analyze "on demand" the characteristic parameters of each family to guide the selection of candidate orbits for missions in the Earth-Moon system. A prototype graphical interface is developed to demonstrate the practical implementation of the dynamic catalog, and can be incorporated into an advanced design environment, such as ATD or GMAT. In particular, the orbits selected through the catalog can be exported for further examination in an end-to-end trajectory design suite. As demonstration, the catalog framework is successfully employed for the preliminary selection of viable orbits for long-term storage infrastructures near the Moon or astrophysical observatories inspired by the IBEX and TESS mission concepts. In addition, the trajectory characteristics that are based on a simplified gravitational model of the Earth-Moon system (i.e. CR3BP) are approximately retained when corrected in an ephemeris model.

VII. Acknowledgements

This work was completed at Purdue University under NASA Grants NNX13AM17G and NNX13AH02G. The authors also appreciate the support of the School of Aeronautics and Astronautics and wish to express their gratitude to Ph.D. candidate Ms. Amanda Haapala and Dr. Thomas Pavlak for their valuable insight and assistance with the computational aspects of this research. In addition, many thanks to Dr. Mar Vaquero for early contributions to this work and Ph.D. student Ms. Lucia Capdevila for valuable discussions.

References

[1]B.G. Drake, *NASA Decadal Planning Team Mars Mission Analysis Summary,* February 2007.

[2]NASA Advanced Development Office, *Lunar L_1 Gateway Conceptual Design Report,* October 2001.

[3]NASA Headquarters, Science Mission Directorate, *NASA Astrophysics Implementation Plan,* December 2012:

[4]International Space Exploration Coordination Group, *The Global Exploration Roadmap,* August 2013.

[5]National Research Council. *Pathways to Exploration: Rationales and Approaches for a U.S. Program of Human Space Exploration.* Washington, DC: The National Academies Press, 2014.

[6]D.C. Folta, M.A. Woodard, and D. Cosgrove, 2011. "Stationkeeping of the First Earth-Moon Libration Orbiters: The ARTEMIS Mission," *AAS/AIAA Astrodynamics Specialist Conference*, Alaska. AAS 11-515.

[7]Satellite ToolKit, Software Package, Analytical Graphics Inc., Exton, PA, 2012.

[8]General Mission Analysis Tool, Available from gmatcentral.org.

[9]E.J. Doedel, V.A. Romanov, R.C. Paffenroth, H.B. Keller, D.J. Dichmann, J. Galán-Vioque and A. Vanderbauwhede, "Elemental Periodic Orbits Associated with the Libration Points in the Circular Restricted 3-Body Problem". *International Journal of Bifurcation and Chaos*, Vol 17, No. 8, 2007.

[10]A. Haapala, M. Vaquero, T.A. Pavlak, K.C. Howell, and D. Folta, "Trajectory Selection Strategy for Tours in the Earth-Moon System," *AAS/AIAA Astrodynamics Specialist Conference*, Hilton Head, South Carolina, August 10-15, 2013.

[11]Farquhar, R.W., Dunham, D.W., Guo, Y., McAdams, J.V., "Utilization of libration points for human exploration in the SunEarthMoon system and beyond," *Acta Astronautica*, Vol. 5, No. 3, 2004, pp. 687–700.

[12]D.G. Yarnoz, J.P. Sanchez and C.R. McInnes, "Pure Opportunities for Asteroid Retrieval Missions," In: *Asteroids*. Springer Berlin Heidelberg, London, Chapter 21. 2013.

[13]K. Uesugi, "Space Odyssey of an Angel: Summary of the HITEN's Three Year Mission". *Advances in the Astronautical Sciences*, Vol. 84, pp. 607-621, 1993

[14]C. D. Murray and S. F. Dermott, "Solar System Dynamics". Cambridge, United Kingdom: Cambridge University Press, Cambridge, 1999.

[15]J. Carrico Jr., D. Dichmann, L. Policastri, J. Carrico III, T. Craychee, J. Ferreira, M. Intelisano, R. Lebois, M. Loucks, T. Schrift and R. Sherman, "Lunar Resonant Trajectory Design for the Interstellar Boundary Explorer (IBEX) Extended Mission," *AAS/AIAA Astrodynamics Specialist Conference*, Girdwood, Alaska, July 31-August 4, 2011.

[16]J.W. Gangestad, G.A. Henning, R. Persinger, G.R. Ricker, "A High Earth, Lunar Resonant Orbit for Lower Cost Space Science Missions," *AAS/AIAA Space Flight Mechanics Meeting*, August 11-15, 2013.

[17]Vaquero, M., and Howell, K., "Leveraging Resonant Orbit Manifolds to Design Transfers between Libration Point Orbits," *Journal of Guidance, Control and Dynamics,* Vol. 37, No. 4, 2014, pp 1143-1157.

[18]N. Strange, D. Landau, T. McElrath, G. Lantoine, T. Lam, M. McGuire, L. Burke, M. Martini, and J. Dankanich, "Overview of Mission Design for NASA Asteroid Redirect Robotic Mission Concept," *International Electric Propulsion Conference*, Washington D.C., October 6-10, 2013.

[19]G. Mingotti, F. Topputo, F. Bernelli-Zazzera, "Exploiting Distant Periodic Orbits and their Invariant Manifolds to Design Novel Space Trajectories to the Moon," *AAS/AIAA Space Flight Mechanics Meeting*, February 14-18, 2010.

[20]T.A. Pavlak, "Trajectory Design and Orbit Maintenance Strategies in Multi-body Dynamical Regimes" Ph.D. Dissertation, School of Aeronautics and Astronautics, Purdue University, West Lafayette, Indiana, 2013.

[21]D. Folta, T. Pavlak, A. Haapala, and K.C. Howell, "Preliminary Considerations for Access and Operations in Earth-Moon L1/L2 Orbits," *AAS/AIAA Space Flight Mechanics Meeting*, Kauai, Hawaii, August 10-14, 2013.

[22]Folta, D., Bosanac, N., Guzzetti, D., and Howell, K., "An Earth-Moon System Trajectory Design Reference Catalog," *2nd IAA Conference on Dynamics and Control of Space Systems*, Roma, Italy, March 24-26, 2014.

[23]W. S. Koon, M. W. Lo, J. E. Marsden, S. D. Ross, *Dynamical Systems, the Three Body Problem and Space Mission Design*. Springer-Verlag New York Incorporated, 2011.

[24]L. Perko, *Differential Equations and Dynamical Systems*. Third Edition, New York, Springer, 2000.

[25]M. Kakoi, K.C. Howell, and D. Folta, "Access to Mars from Earth-Moon Libration Point Orbits: Manifold and Direct Options," *Acta Astronautica*, Vol. 102, September-October 2014, pp. 269-286.

[26]L. Capdevila, D. Guzzetti, and K.C. Howell, "Various Transfer Options from Earth into Distant Retrograde Orbits in the Vicinity of the Moon," *AAS/AIAA Space Flight Mechanics Meeting*, January 26-30, 2014.